PULSE SHAPED CONSTANT ENVELOPE 8-PSK MODULATION STUDY

Jianping Tao
Sheila Horan

NMSU-ECE-97-005 **March 1997**

THE KLIPSCH SCHOOL OF

ELECTRICAL AND COMPUTER ENGINEERING

TECHNICAL REPORT SERIES

PULSE SHAPED CONSTANT ENVELOPE 8-PSK MODULATION STUDY

Jianping Tao
Sheila Horan

NMSU-ECE-97-005 March 1997

PULSE SHAPED CONSTANT ENVELOPE 8-PSK MODULATION STUDY

Jianping Tao
Sheila Horan

Supported by NASA Grant #NAG5-1491

NMSU-ECE-97-005

March 1997

TABLE OF CONTENTS

LIST OF TABLES

LIST OF FIGURES

LIST OF ABBREVIATIONS

α	Rolloff Factor for SRRC filters
ρ	Band Utilization Ratio
AWGN	Additive White Gaussian Noise
ASCII	American Information Code for Information Interchange
dB	Decibels
BER	Bit Error Rate
Bi-ϕ	Bi-Phase (Manchester)
BPSK	Binary Phase Shift Keying
BW	Bandwidth
BT	Bandwidth-Time (symbol) product
CCSDS	Consultative Committee for Space Data Systems
DC	Direct Current
Eb/No	Energy (bit) to Noise ratio
ESA	European Space Agency
f_s	Sampling Frequency
FFT	Fast Fourier Transform
FSE	Fractionally Spaced Equalizer
FSK	Frequency Shift Keying
Hz	Hertz
HP	Hewlett Packard
IF	Intermediate Frequency
IIR	Infinite Impulse Response (filter)
ISI	Intersymbol Interference
JPL	Jet Propulsion Laboratory
LMS	Least Mean Squared
LSB	Least Significant Bit
MFB	Matched Filter Bank
MLSD	Maximum-Liklihood Sequence Detector
MSB	Most Significant Bit
MSK	Minimum Shift Keying
NASA	National Aeronautics and Space Administration

NMSU	New Mexico State University
NRZ-L	Non-Return-to-Zero Logic
OQPSK	Offset Quaternary Phase Shift Keying
PA	Power Amplifier
PCM	Pulse Coded Modulation
PM	Phase Modulation
PSD	Power Spectral Density
PSK	Phase Shift Keying
QPSK	Quartenary Phase Shift Keying
R_B	Bit Rate
R_S	Symbol or Baud Rate
RC	Raised Cosine
RF	Radio Frequency
sec	Seconds
SF	Single Filter
SFCG	Space Frequency Coordination Group
SNR	Signal-to-Noise Ratio
SPW	Signal Processing Worksystem
SSPA	Solid State Power Amplifier
SRRC	Square Root Raised Cosine
T_B	Bit Period
TWT	Traveling Wave Tube
TWTA	Traveling Wave Tube Amplifier

INTRODUCTION

This report provides simulation results for constant envelope pulse shaped 8 Level Phase Shift Keying (8 PSK) modulation for end to end system performance. In order to increase bandwidth utilization, pulse shaping is applied to signals before they are modulated. This report provides simulation results of power spectra and measurement of bit errors produced by pulse shaping in a non-linear channel with Additive White Gaussian Noise (AWGN). The pulse shaping filters can placed before(Type B) or after(Type A) signals are modulated. Three kinds of baseband filers, 5th order Butterworth, 3rd order Bessel and Square-Root Raised Cosine with different BTs or roll off factors, are utilized in the simulations.

The simulations were performed on a Signal Processing Worksystem(SPW). This project is conducted at New Mexico State University (NMSU) in the Space Communication and Telemetry Laboratory in the Electrical and Computer Engineering Department.

BACKGROUND

The most bandwidth-efficient communication methods are imperative in coping with the congested frequency bands. Pulse shaping methods have excellent effects for narrowing the bandwidth and increasing band utilization. For 8 PSK, a non constant envelope spectrum shaping method was previously simulated [5]. In these simulations, the spectrum of filtered non-constant envelope 8PSK spreads as the signals go through the Solid State Power Amplifier(SSPA). The position of the baseband filters for the pulse shaping are crucial, since if the filter is after the modulator(this will be referred to as type A) and before the modulator(this will be referred to as type B) have different effects for narrowing the bandwidth and producing bit errors. The constant envelope 8 PSK and pulse shaping filters(Type B) are used to perform the simulations on spectrum and bit error rates in this project.

PROCEDURE

8 PSK Theoretic Analysis And Pulse Shaping Methods

This project provides an end to end simulation system. The random binary signal is combined via a Gray code. Then the 8-level signal passes through a pulse shaping filter, is modulated, passed through a channel and then a receiver. Figure 1 shows the system architecture.

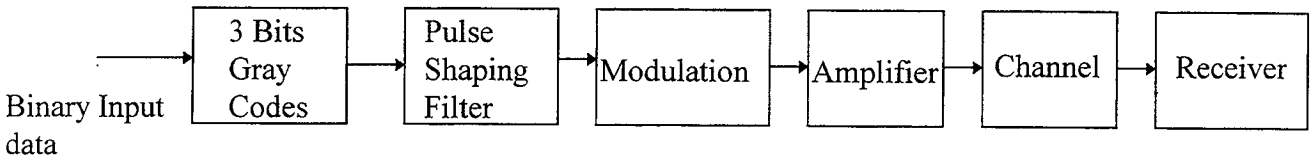

Figure 1 8PSK End To End System Block Diagram

8 PSK Modulation And Pulse Shaping Filters

In 8 level Phase-Shift Keying, information is contained in the phase, and one symbol has 3 bits. The phase of the carrier can take one of 8 discreet equally spaced values, such as $22.5^{\circ},67.5^{\circ},112.5^{\circ},157.5^{\circ},202.5^{\circ},247.5^{\circ},292.5^{\circ},337.5^{0}$. An 8 PSK signal, s(t), can be expressed as follows:

$$s(t)=A_c\exp[j(w_ct+\theta)]=A_c\cos[w_ct+\theta(t)]+jA_c\sin[w_ct+\theta(t)]$$

Where the envelope A_c is constant in this project, $w_c=2\pi f_c$, where f_c is the carrier frequency in hertz, and θ is the phase which takes one of the 8 discrete values in degree corresponding to the 3 bits Gray code. Table 1 shows the relationship between Gray codes and θ.

Binary Gray Codes	θ (Degree)
000	22.5°
001	67.5°
011	112.5°
010	157.5°
110	147.5°
111	247.5°
101	292.5°
100	337.5°

Table 1 Gray Codes And Phase

In SPW, the Gray codes and phase θ can be produced by the design shown in Figure 2.

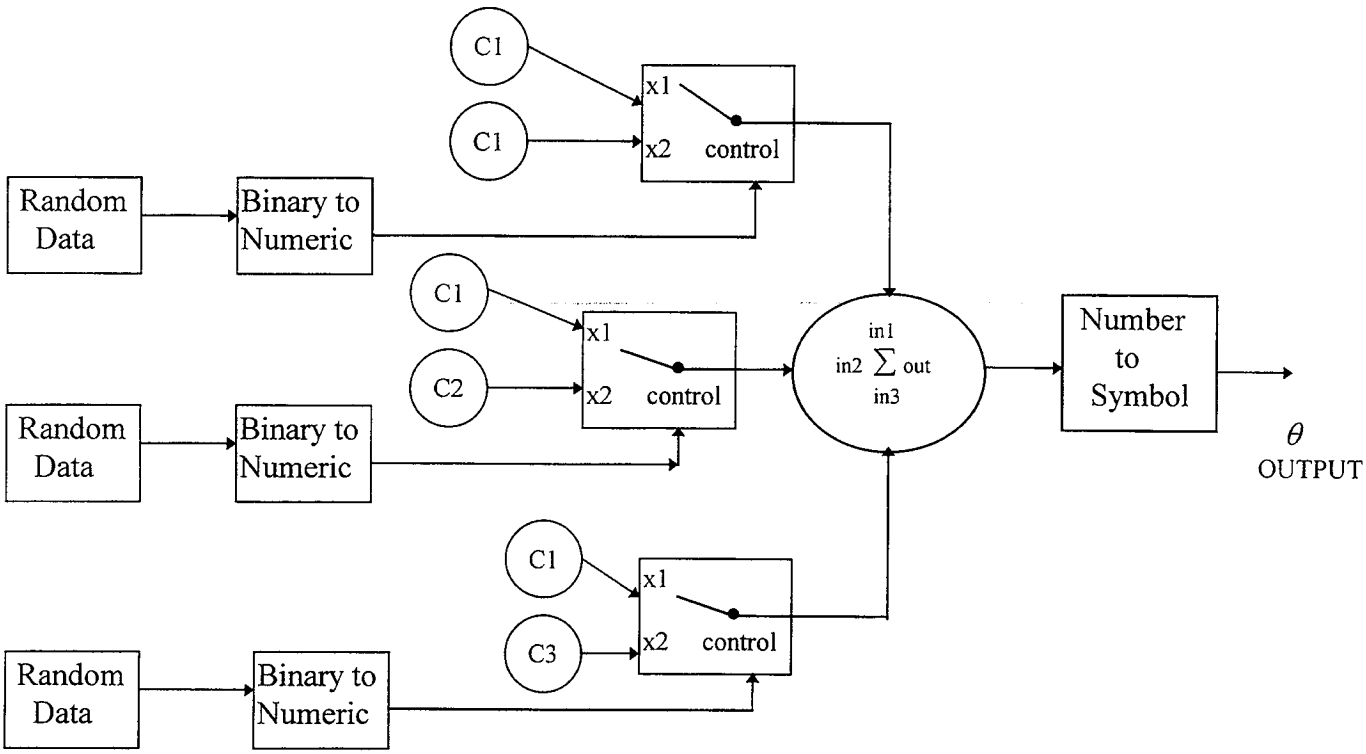

Figure 2 Producing Phase Signals Block Diagram

Where C1=1, C2=2, and C3=4. The Number to Symbol block which has the function as Table 1 completes the conversion from Gray codes to phase in degrees.

NRZ-L Ideal Data and phase signal θ waveform

Binary ideal data is used throughout the simulations. For the ideal data, the logic 0 and 1 have the same probability , it has a perfect symmetry(the duration of a digital one is equal to the time duration of a digital zero). Figure 3 shows the NRZ-L ideal binary data and waveforms of phase θ (in radians)

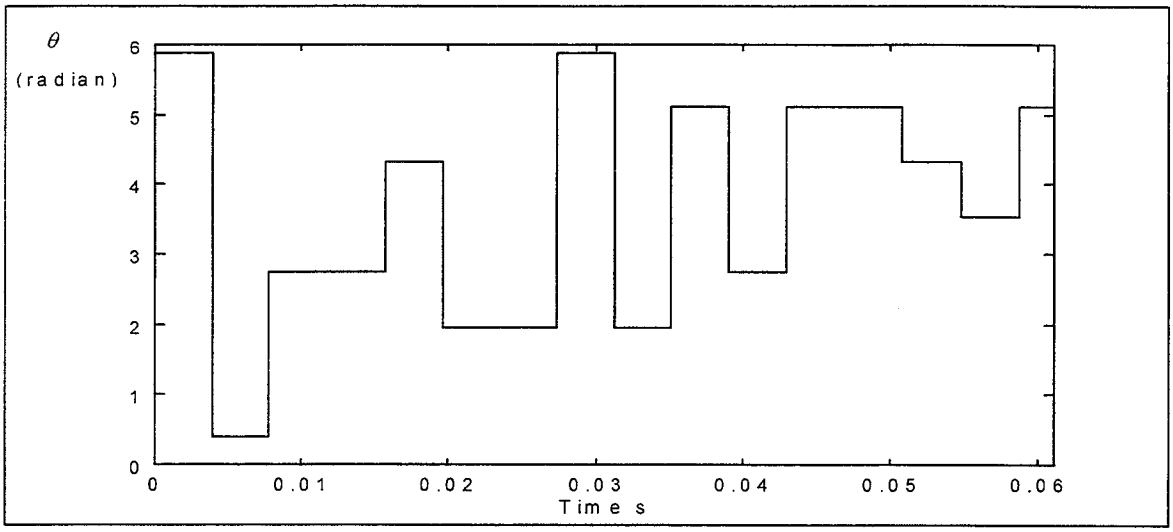

Figure 3 Phase Signals θ Waveform

Modulation

The phase signal shown in Figure 3 can be modulated to an 8 PSK signal, s(t). To realize spectrum shaping, the phase signal, θ, goes through a pulse Shaping filter before being modulated(type B). In this project, Bessel, Butterworth, and Square Root Raised Cosine filters are used. In addition, the change of the position of pulse shaping filters can produce a change of simulation results. If the filter is put behind the modulation[5], type A is simulated. This report will make a comparison to these two types of pulse shaping methods. Figure 4 shows the modulation scheme for unfiltered and filtered 8 PSK signals.

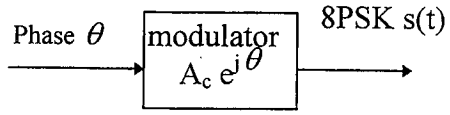

(a) Unfiltered 8PSK With Constant Envelope

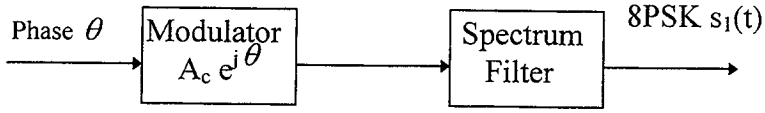

(b) Filtered 8PSK Type A With Non-Constant Envelope

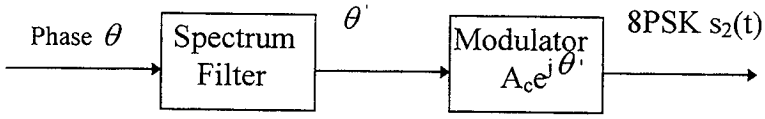

(c) Filtered 8PSK Type B With Constant Envelope A_c

Figure 4. Modulation schemes for unfiltered and filtered phase signals.
(b) is used in this project simulation.

Pulse Shaping Filters

Pulse Shaping Filters are used to narrow bandwidth and improve bandwidth utilization. In this report several types of filters such as 5th order Butterworth, 3rd Order Bessel and Square Root Raised Cosine (SRRC)(α=1) are utilized in the simulations for the ideal data.

Pulse shaping can induce distortions of 8 PSK signals and increase the risk of Inter-Symbol Interference (ISI)[4]. The distortions due to the pulse shaping filters make the design of an optimal receiver difficult.

Butterworth filters: Butterworth filters provide the maximally flat response at Ω=0 and $\Omega=\infty$. Response varies monotonically during the stopband, decreasing smoothly from Ω=0 and $\Omega=\infty$. In the simulation, The 5th Order Butterworth filter is used.

Bessel Filters: The Bessel type of filter has the slowest transition between passband and stopband and the passband phase response is better than the Butterworth. It has approximately linear phase in the passband so that it has a property of preventing

dispersion of the signal. The amplitude for Bessel filters is not as flat in the passband region as for the Butterworth filters. This project uses a 3rd Order Bessel Filter for the simulation.

Square Root Raised Cosine Filter (α=1) The Square Root Raised cosine filter obtains the filter coefficients according to the following formula[1]:

$$h(t)=4\alpha\frac{[\cos((1+\alpha)\pi\frac{t}{T})+\sin((1-\alpha)\pi\frac{t}{T})]}{\pi\sqrt{T}[(4\alpha\frac{t}{T})^{2}-1]}$$

In this equation, α is the roll off parameter and T is one symbol period(1/symbol rate). The Real Raised cosine block in SPW is selected for the project simulation. As mentioned in [5], if the Raised cosine filters are used the ISI will be eliminated in a linear channel. The SRRC filtering is noncausal and has infinite coefficients, but actually a finite number of coefficients are needed to determine the FIR tap length. This truncation can cause some frequency distortion. On the other hand, the distortion can be reduced by applying any of several windowing functions such as Bartlett, Blackman, or Hamming. However, filtering occurs before modulation, the channel is no longer linear as far as the filter is concerned.

The Observation Of Unfiltered And Filtered 8 PSK Signals

With the use of pulse shaping filters, the 8 PSK signals change their shape. The main character of the waveform change is a transient(rise and drop) in the filtered θ' (as shown in Figure 5). The transient line(rise or drop) makes a big difference between unfiltered(as shown in Figure 6) and the filtered 8PSK shown in Figure 7.

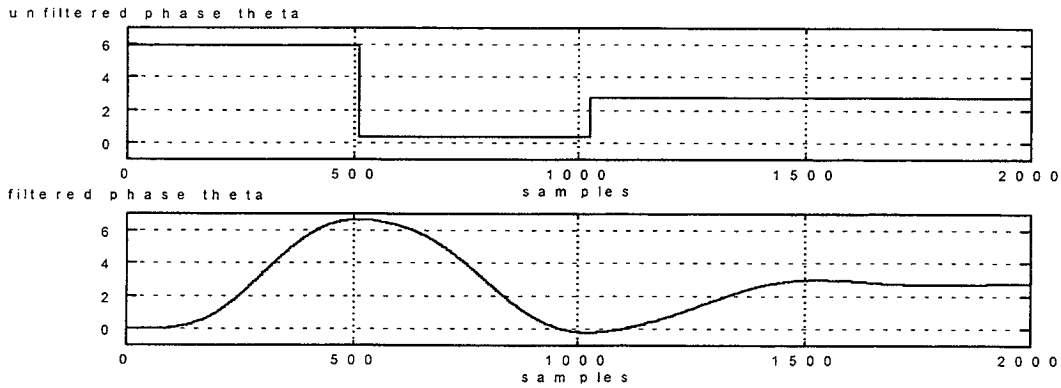

Figure 5 The Waveforms Of Unfiltered θ And Filtered θ'
(Butterworth 5th filter is used, BT=1)

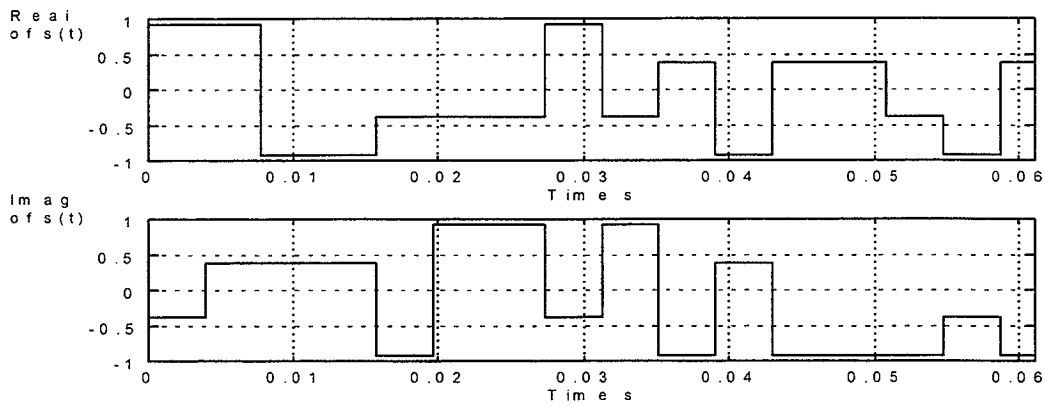

Figure 6 Real Part And Imaginary Part Of Unfiltered 8 PSK For Ideal Data

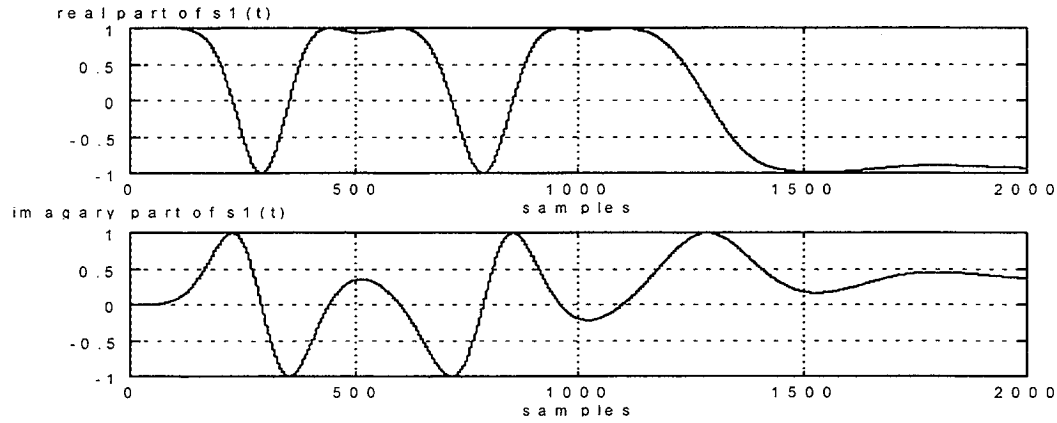

Figure 7 Real Part And Imaginary Part Of Filtered 8 PSK Type B (512 Samples/Symbol)

From Figures 5 and Figure 7, it can be seen that the filtered phase θ has a transient from 0 to 2 π . In sample range 0 to 500, the waveform of the filtered 8 PSK has a tremendous change in that transient range. It changes from a constant to a sinusoid wave. The reason for this change is the Intersymbol Interference(ISI) introduced by the filtering process. The filtering process elongates data symbols such that they overlap one another. When the pulse waveforms pass through the bandlimited system, they will be spread or dispersed. This spreading can cause ISI which increases error rates and affects power spectrum.

Solid State Power Amplifier(SSPA)

A Solid State Power Amplifier (SSPA) is used in the project. The magnitude and phase plots of the SSPA were obtained from JPL. From the plot(Figure 8), the SSPA has two main ranges which include a linear and non-linear region. If the input power is less than -5 dB, the SSPA is worked in the linear region, and the phase offset is approximately zero. If the input power is larger than -5 dB, the SSPA is working in the nonlinear region. This project sets the SSPA to work at saturation level of 0 dB.

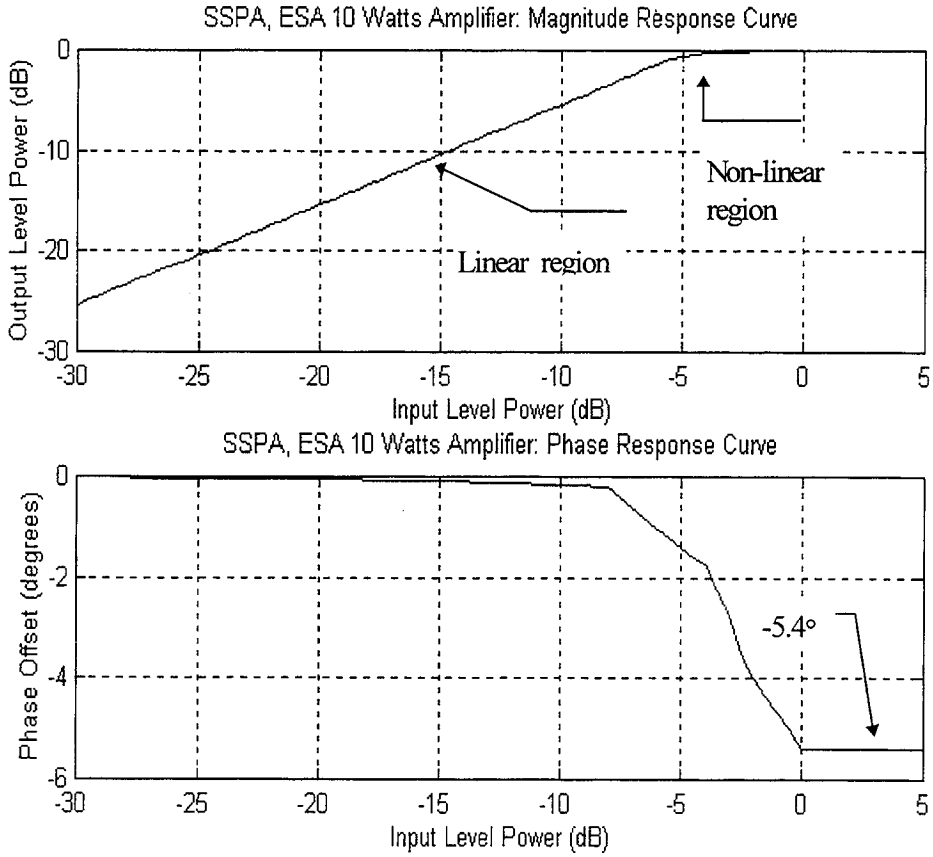

Figure 8 The Output Characteristic Of 10 Watts SSPA

The main part of the SSPA is an analytical Traveling Wave Tube (TWT) block which can simulate the nonlinear channel. By looking up the SSPA table file provided by JPL, the TWT realizes a conversion from input amplitude to output amplitude and input amplitude to out phase. Figure 9 shows the structure of the SSPA.

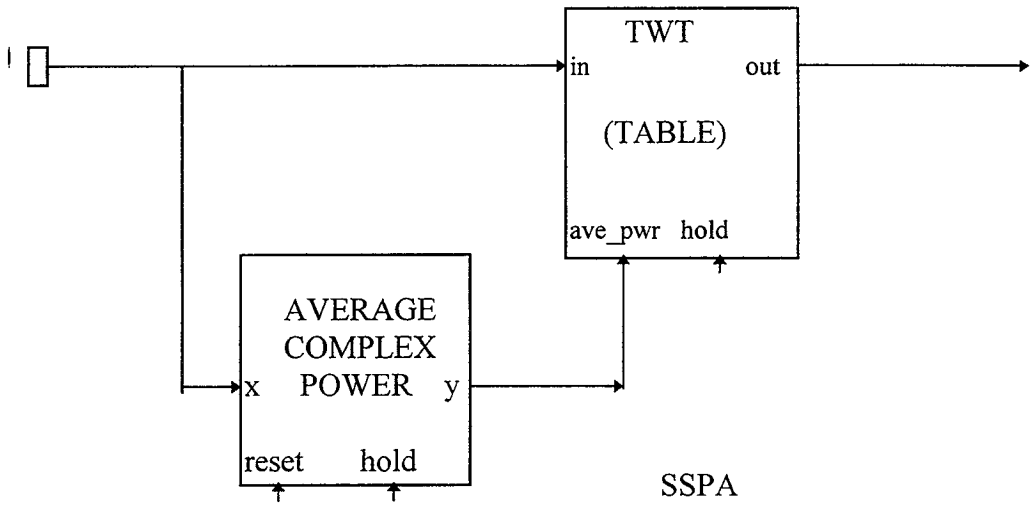

Figure 9 The Structure of SSPA.

Power Spectra Analysis

Figure 10 shows the procedure for obtaining the power spectra for 8 PSK signal.

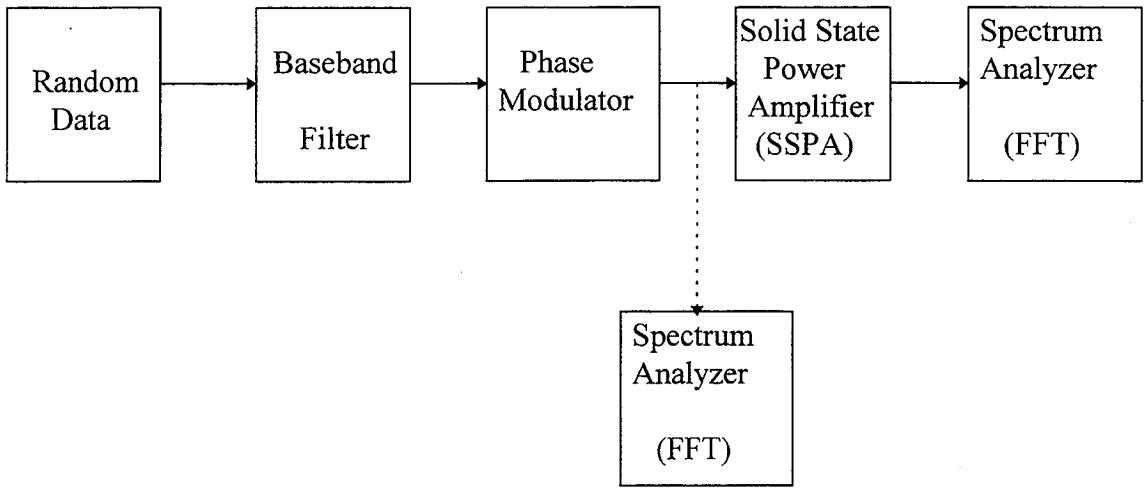

Figure 10 Block Diagram of Spectrum Analysis

The random data source provides ideal data with a data rate of 256 Hz, and the sample frequency, Fs, is 131072 Hz. For the spectrum shaping, three types are used. They are 5th order Butterworth with BT=1, 2, 2.8, 3, 3rd order Bessel with BT=1, 1.2, 2, 3, and square-Root Raised Cosine with roll off factor α =1. The BT represents the product of the bandwidth with the symbol time. The constant envelope 8 PSK signal which comes from the modulator goes to the input of the Solid State Power Amplifier(SSPA).

The spectrum Analyzer can be put before and after the SSPA. Since the SSPA is worked at the saturation level and constant envelope 8PSK is used, the spectrum of the signal at the input of the SSPA is almost the same as that of the signal output from the SSPA. The Spectrum Analyzer is picked up from Interactive Simulation Library(ISL) of SPW. The power spectrum is obtained by taking the Fast Fourier Transform(FFT)of the input signals of the Spectrum Analyzer. The FFT length is 131072, and the window is Bartlett. The power spectrum is produced by taking 100 FFTs averaged together. The plot on the ISL window can be copied to the Signal calculator window by using Ctr-D. It is worthwhile to mention that the scaling on the vertical axis is relative. Suppose the vertical axis on the window is from 0 to -100 dB and the scale on the signal calculator window is -1 to 1, one can obtain the relationship by using following formula

$$S2=(S1-1)*50$$

Where S1 is the value on the signal calculator window, and S2 is the actual value.

Additive White Gaussian Noise Channel

Additive White Gaussian Noise(AWGN) is added to the signals out of the SSPA to simulate channel noise. Figure 11 shows the power spectral density for the AWGN used in the simulations. Actual white noise has a flat spectrum from $-\infty$ to ∞.

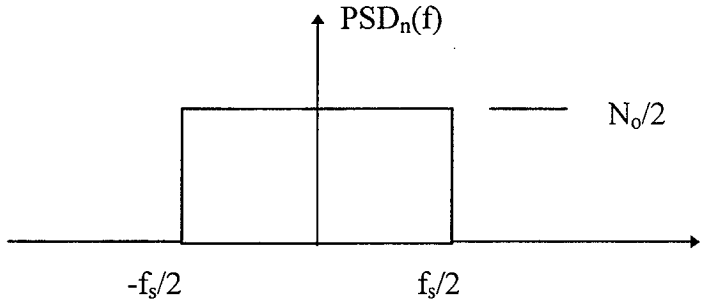

Figure 11 Power Spectral Density Of White Noise.

The AWGN is taken to have zero mean and with variance σ_n^2 =N_o/2. N_0/2 is the power spectral density of the white noise, and F_s is the sampling frequency.

Receiver And Error Rate Estimation System

There are three parts in the receiver and estimation system. These are the receiver(matched filter),synchronizer and error rate estimator. Figure 13 shows the block diagram for this system.

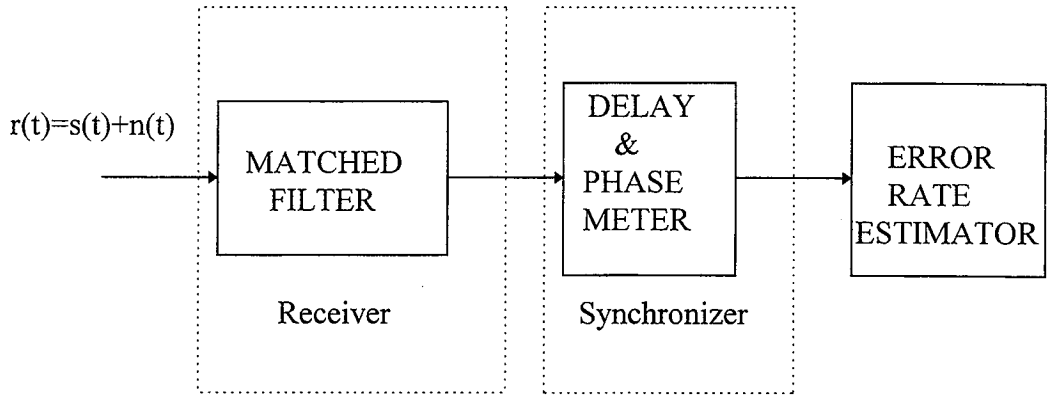

Figure 12 Block Diagram For The Receiver Error Rate Estimator

Receiver

A matched filter is ideally used as a receiver. The matched filter is a linear filter which minimizes the noise and maximizes the signal. In this project, an integrate and dump block is used as the matched filter(matching to the NRZ data). Since the actual signal is fairly complex(due to the pulse shaping),a truly matched filter was not attempted at this time.

Synchronizer

The synchronizer performs a correlation between the reference signals and the received signals(delayed and distorted), and gives an estimate of the number of samples of delay and the phase between the two samples. The reference signal is then delayed the same number of samples so that the two signals can be compared to get the error rate. Figure 13 shows the block diagram for the synchronization. The DELAY & PHASE METER can detect the number of sample delays of the received signals. The COMPLEX VARIABLE DELAY lets the reference signals be delayed by the same number of samples as the received signal so they can be compared in the error rate estimator.

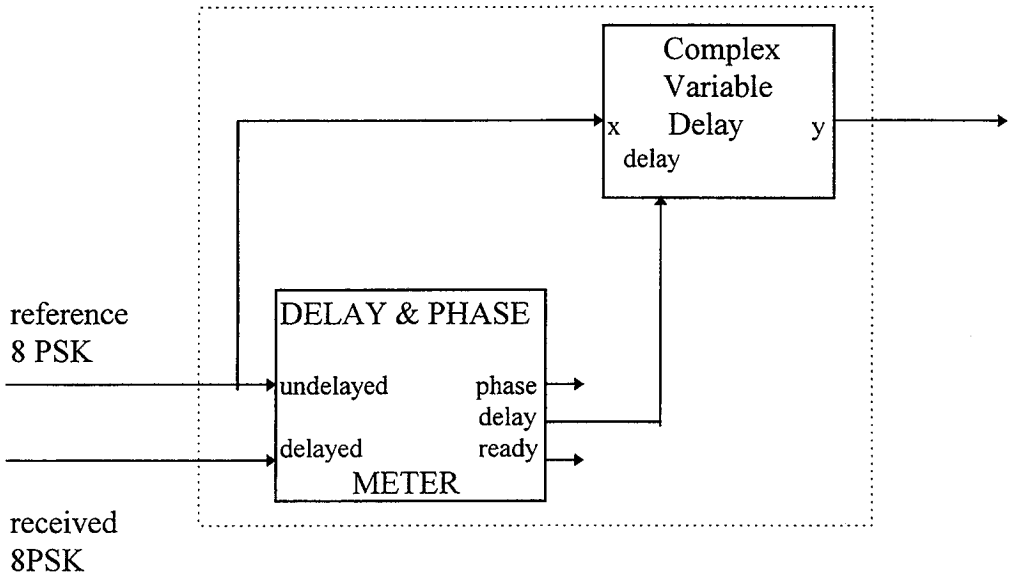

Figure 13 Block Diagram of Synchronizer

Error Rate Estimator

The reference signal and received signal now having the same delay, are put into the error rate estimator to count the number of bit errors. The main block used to count bit errors is SIMPLE ERROR RATE ESTIMATOR(Figure 14)which compares the reference and the received signals to find bit errors.

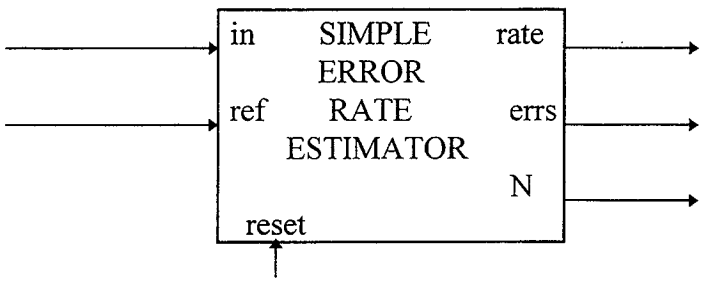

Figure 14 Simple Error Rate Estimator Block Diagram

SIMULATIONS

Figure 15 shows the system block diagram for the 8 PSK end to end system simulations. The simulations include two main parts: Power Spectrum and Bit Error Rates.

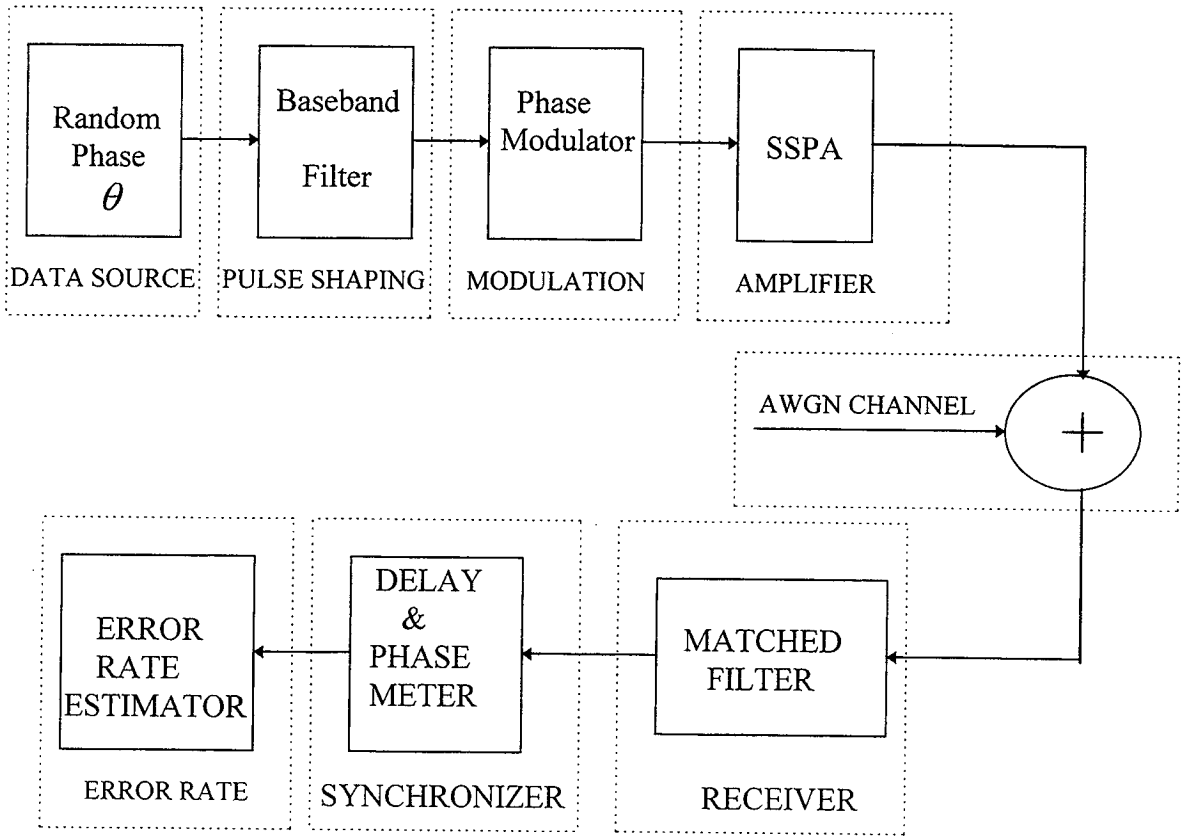

Figure 15 Simulation System Block Diagram

Simulations on Power Spectrum

Figure 10 showed the location of where to obtain the power spectrum. The following parameters were used to obtain the power spectra.

Data Source:

a. Ideal data with p(0)(probability of zero)=0.5;
b. Sample Rate (f_s) = 131072 Hz
c. Symbol rate R_s=256 (Bit rate=768; 512 samples/symbol);

Base band Filters

a. None
b. Butterworth 5th Order (BT=1,2,2.8,3)

c. Bessel 3rd Order (BT=1,1.2,2,3)

d.SRRC(α =1, Number of tap length=16*512=8192, Bartlett window, Square-root raised cosine='yes'; Sample input='yes')

Power Amplifier:

European Space Agency(ESA) 10-watt SSPA

SPW Spectrum Analyzer

a. FFT length=131072

b. Window type: Bartlett

c. Average: 100 FFTs

d. Sampling frequency =131072

Spectrum Plots ranges

$\pm 10\ R_b$; $\pm 75\ R_b$; $\pm 250\ R_b$

The plots of the power spectra are given in Figures 16-34.

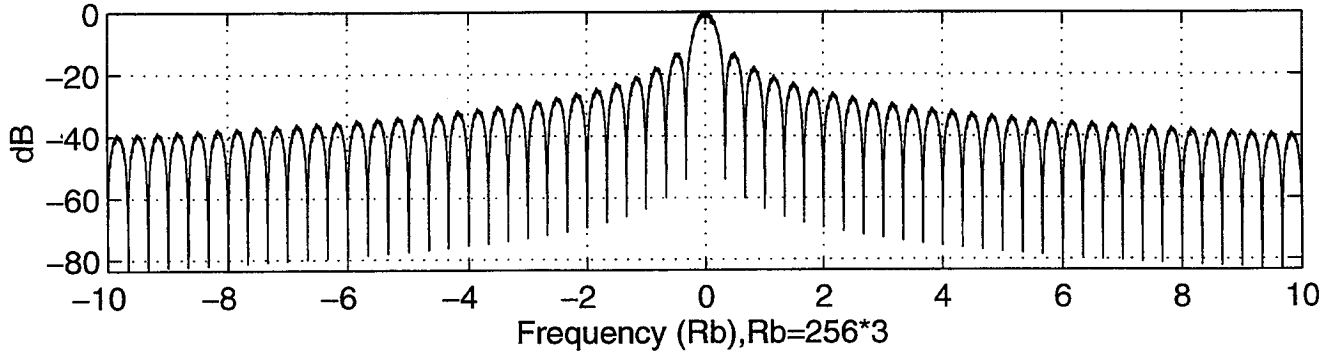

(a) Unfiltered 8 PSK $\pm 10\ R_b$

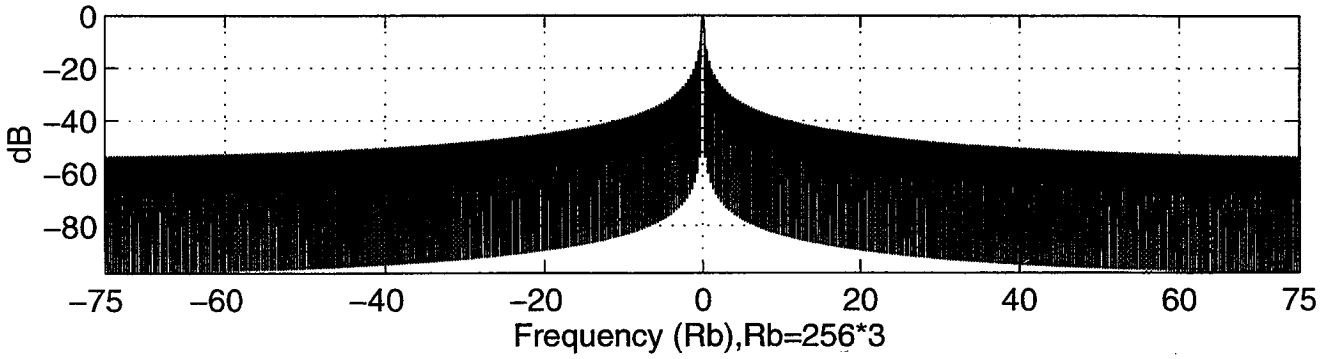

(b) Unfiltered 8 PSK $\pm 75\ R_b$

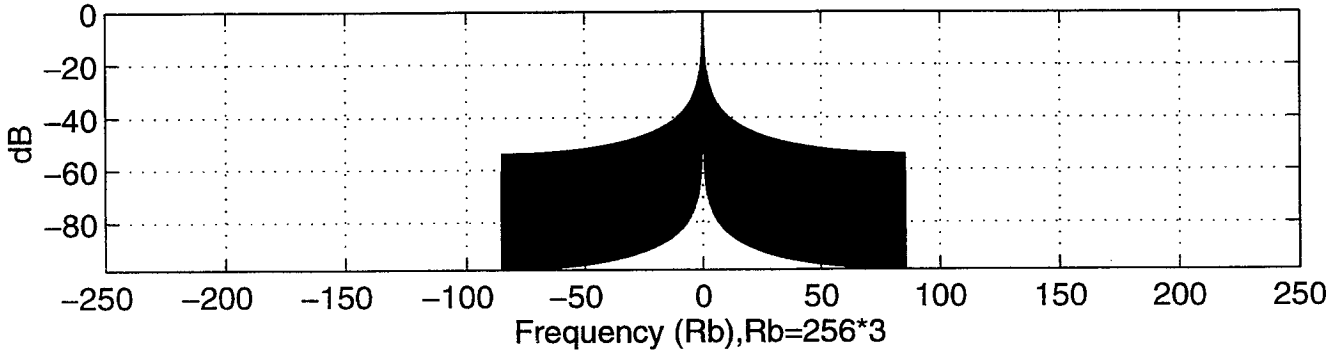

(c) Unfiltered 8 PSK $\pm 250\ R_b$

Figure 16: Unfiltered Power Spectral Density

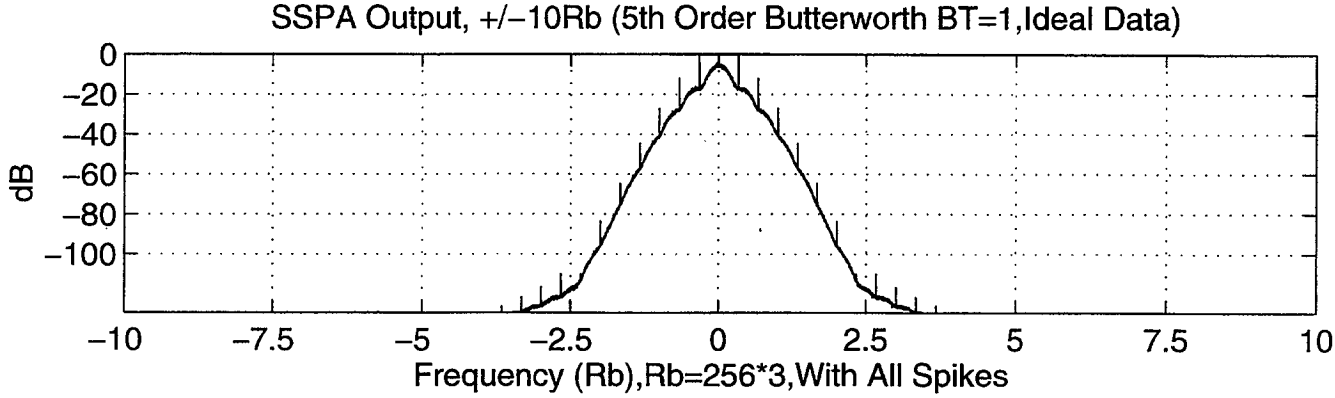

(a) 5th Order Butterworth Filter (BT=1), $\pm 10\ R_b$

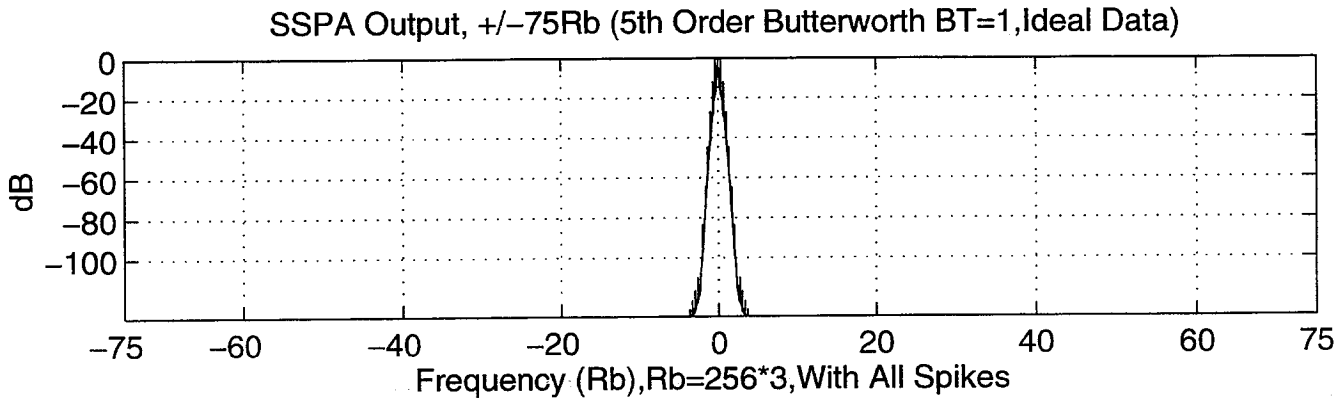

(b) 5th Order Butterworth Filter (BT=1) , $\pm 75R_b$

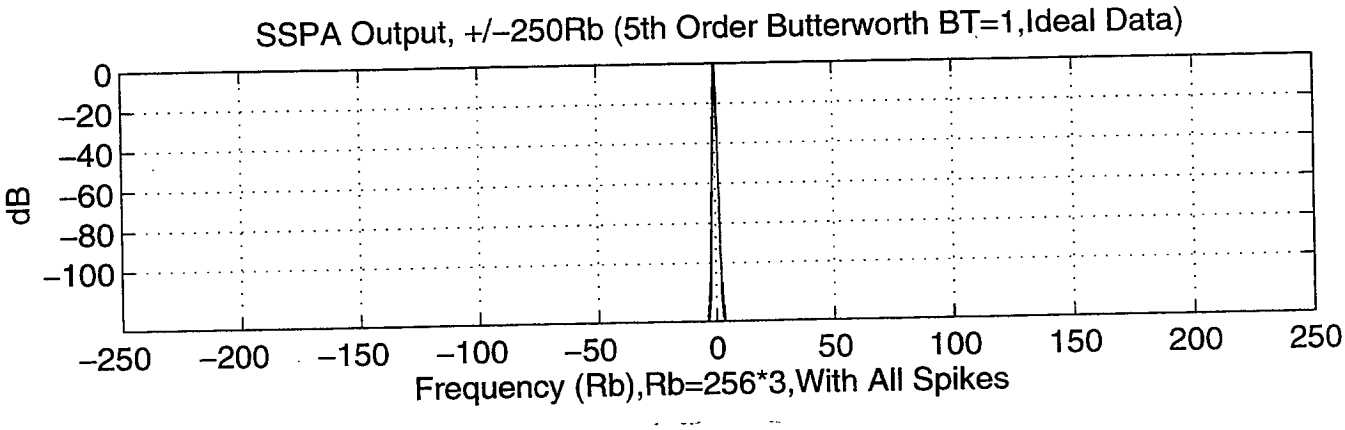

(c) 5th Order Butterworth Filter (BT=1), $\pm 250R_b$

Figure 17: 5th Order Butterworth Filter (BT=1) Power Spectra, With Central Spike

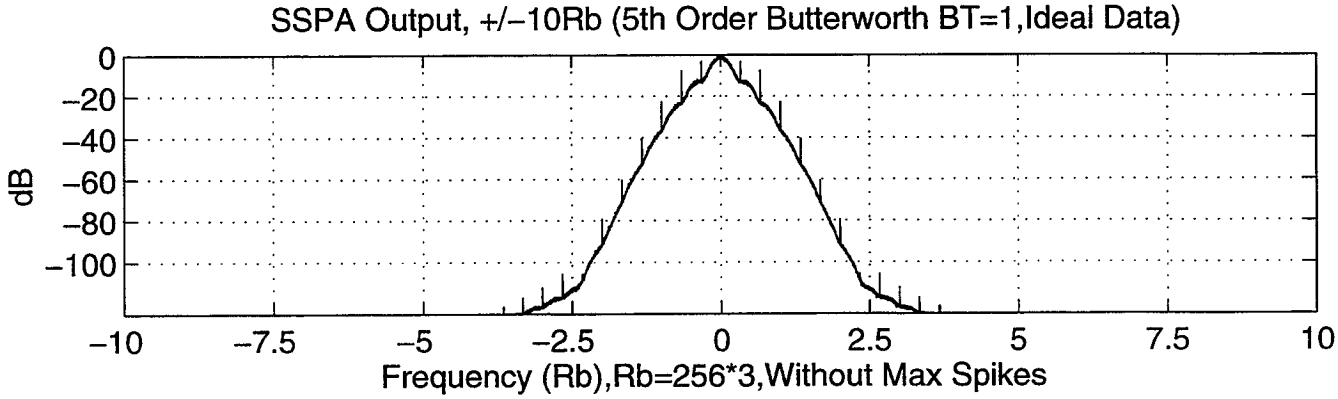

(a) 5th Order Butterworth Filter (BT=1), $\pm 10\ R_b$

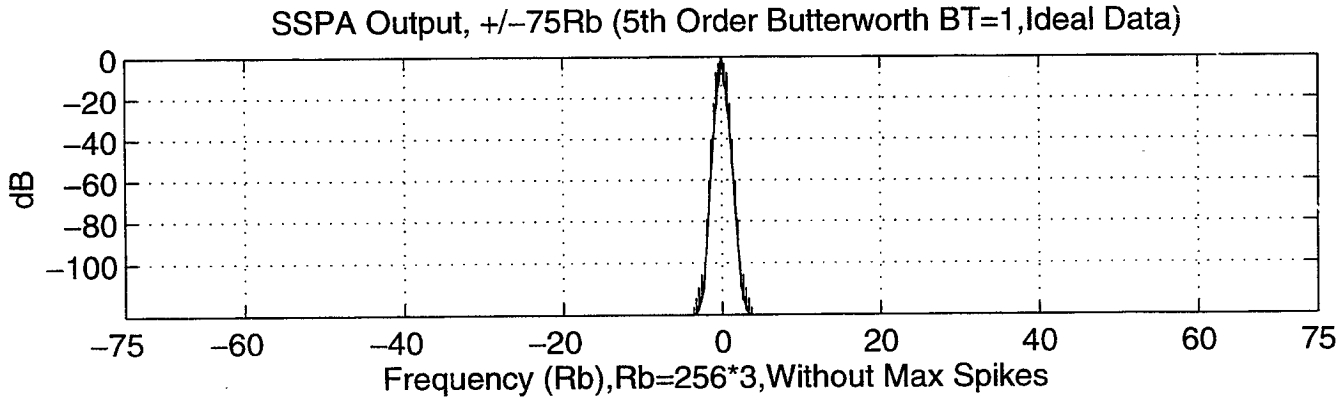

(b) 5th Order Butterworth Filter (BT=1) , $\pm 75R_b$

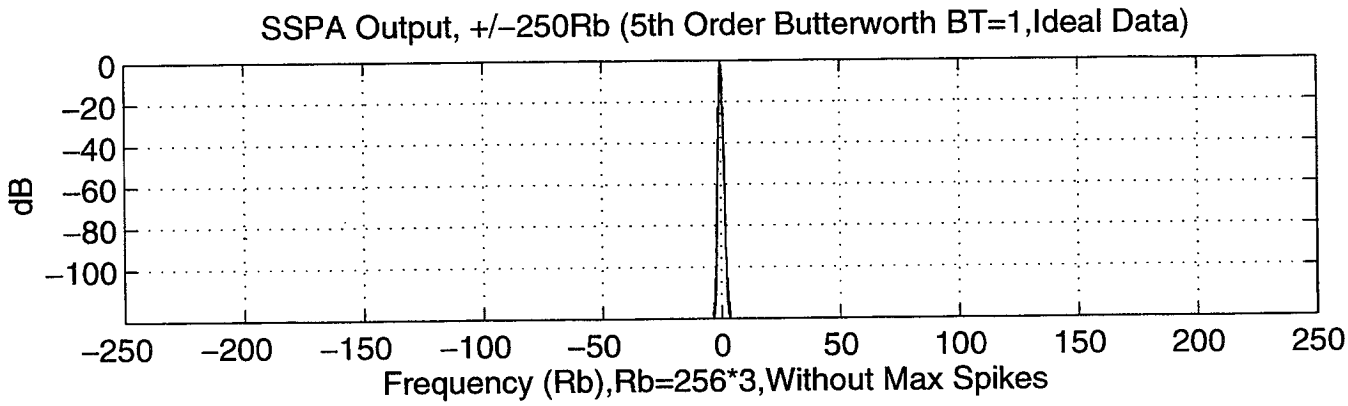

(c) 5th Order Butterworth Filter ,BT=1, $\pm 250R_b$

Figure 18: 5th Order Butterworth Filter Power Spectra, Without Central Spike

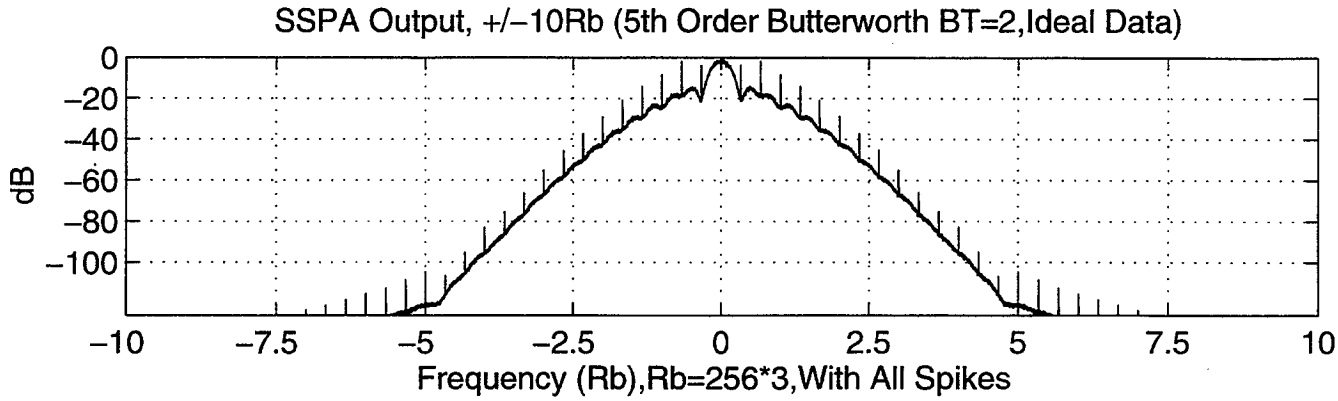

(a) 5th Order Butterworth Filter (BT=2) , $\pm 10R_b$

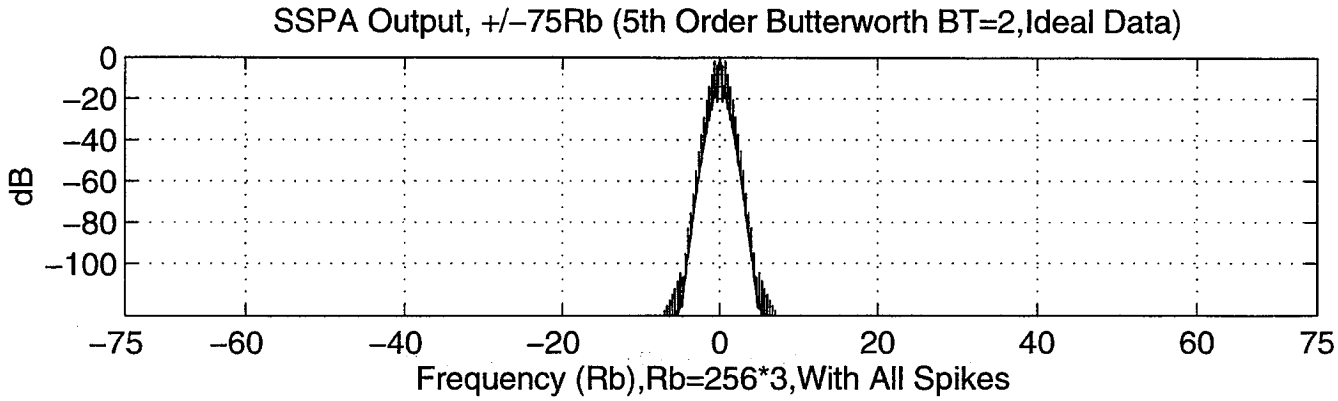

(b) 5th Order Butterworth Filter (BT=2) , $\pm 75R_b$

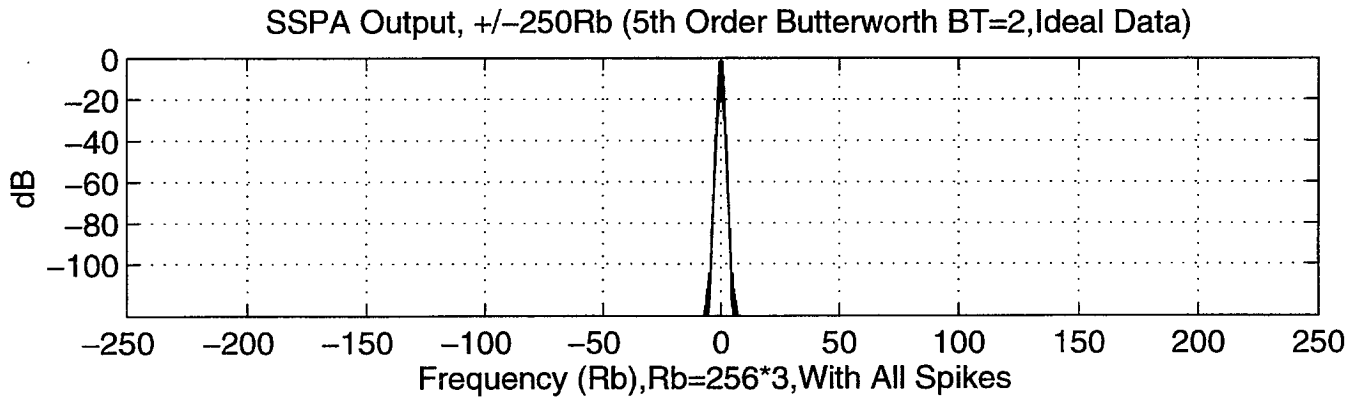

(c) 5th Order Butterworth Filter (BT=2), $\pm 250R_b$

Figure 19: 5^{th} Order Butterworth Filter (BT=2) Power Spectra, With Central Spike

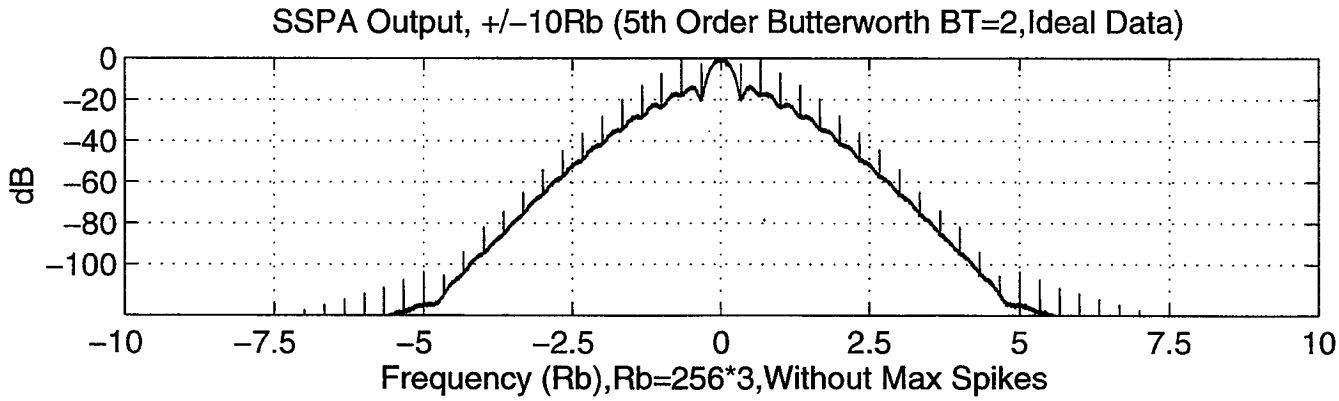

(a) 5th Order Butterworth Filter (BT=2) , $\pm 10R_b$

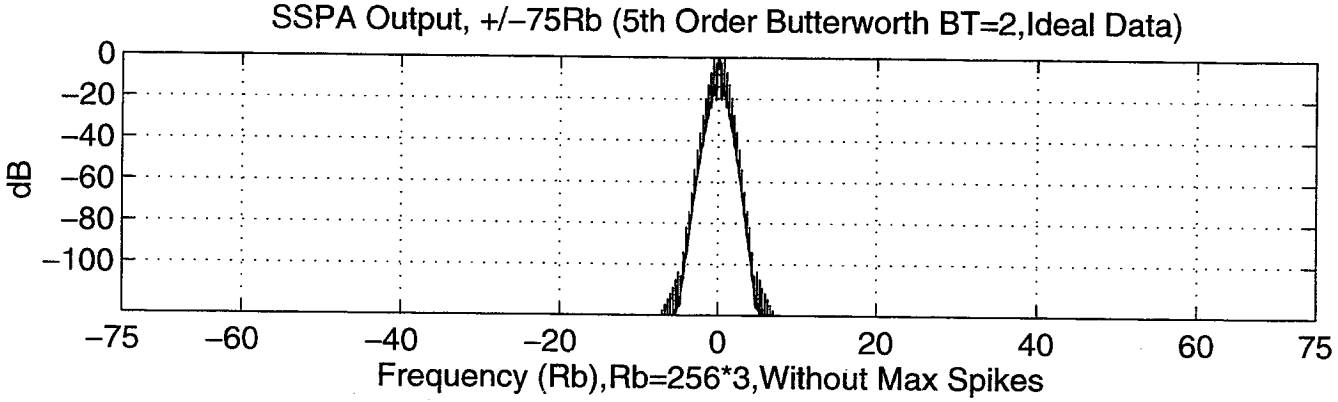

(b) 5th Order Butterworth Filter (BT=2) , $\pm 75R_b$

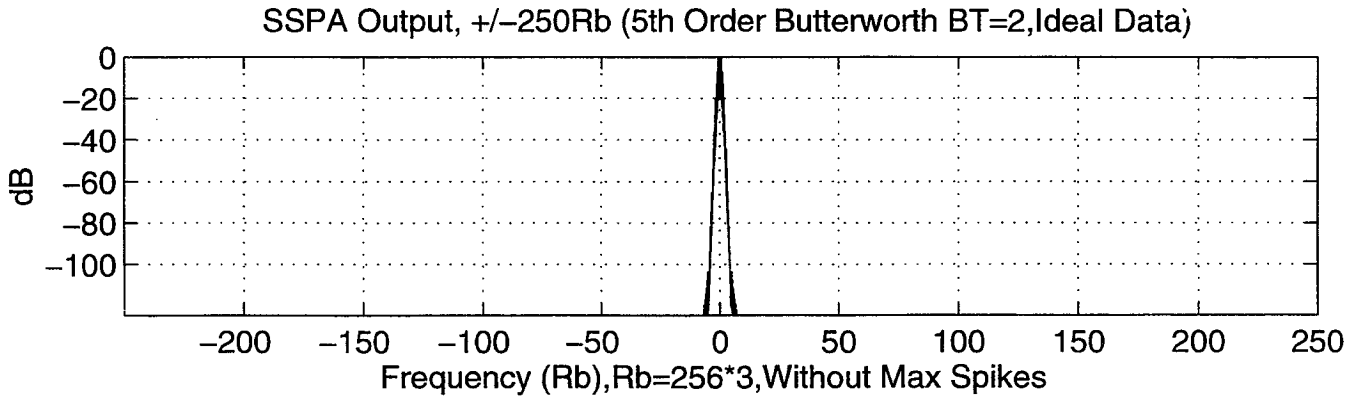

(c) 5th Order Butterworth Filter (BT=2), $\pm 250R_b$

Figure 20: 5^{th} Order Butterworth Filter (BT=2), Without Central Spike

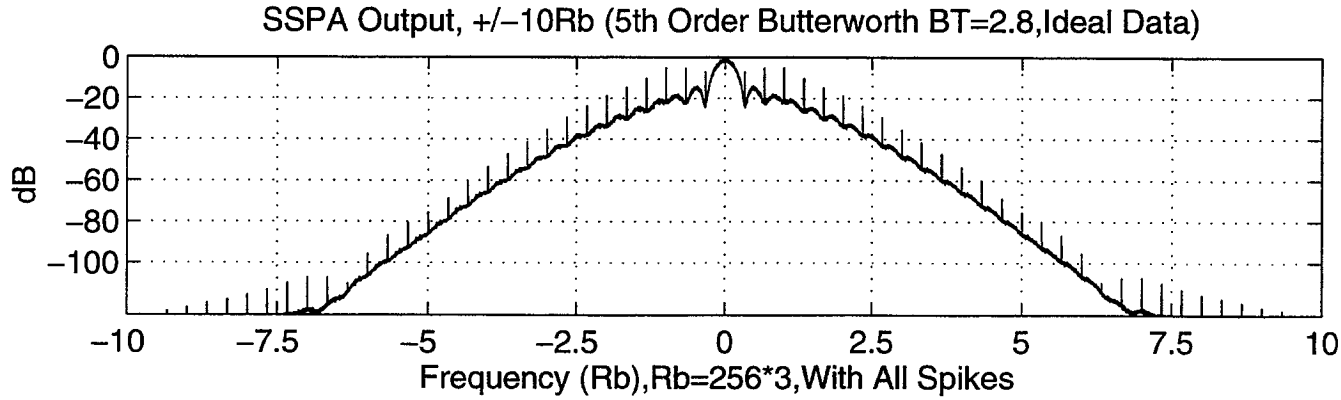

(a) 5th Order Butterworth Filter (BT=2.8), $\pm 10R_b$

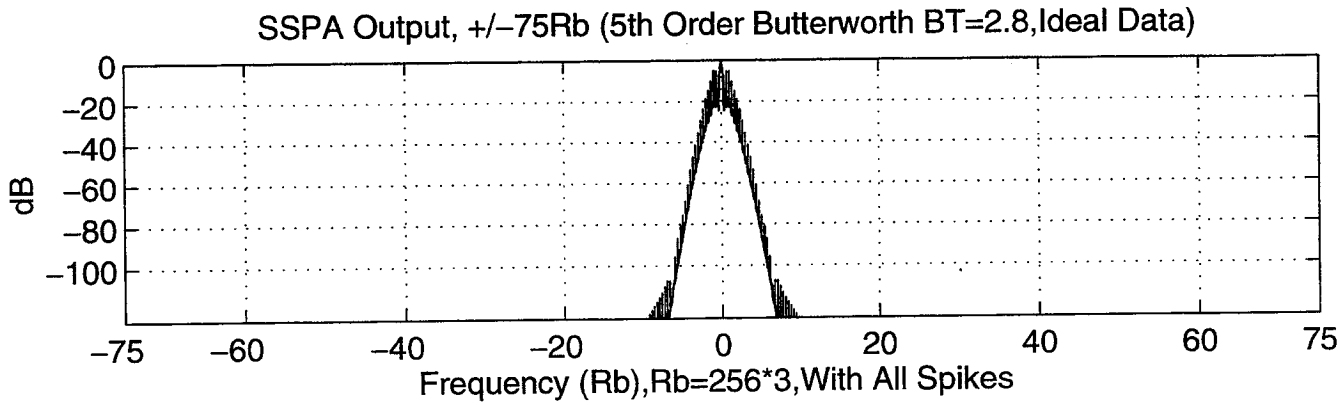

(b)5th Order Butterworth Filter (BT=2.8), $\pm 75R_b$

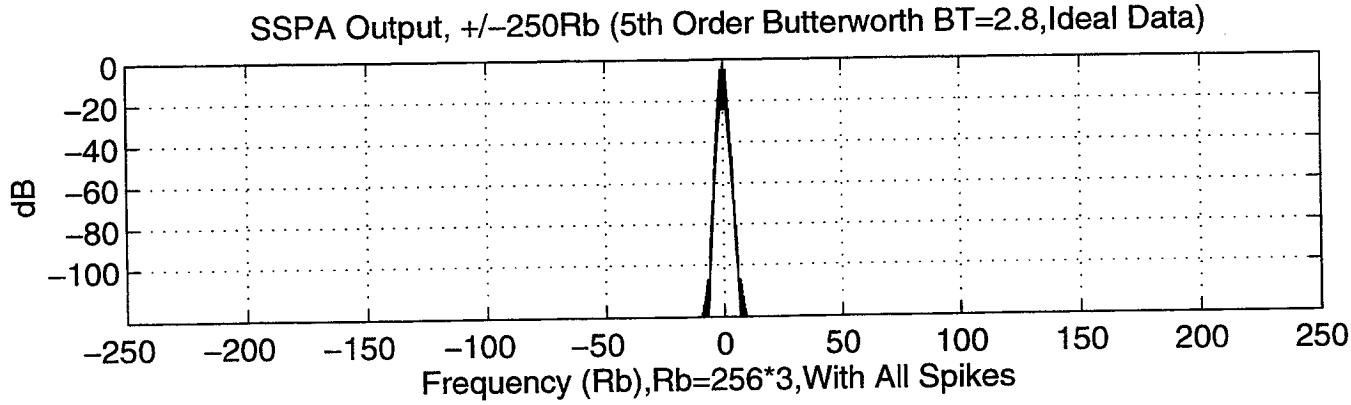

(c) 5th Order Butterworth Filter (BT=2.8), $\pm 250R_b$

Figure 21: 5th Order Butterworth Filter (BT=2.8) Power Spectra, With Central Spike

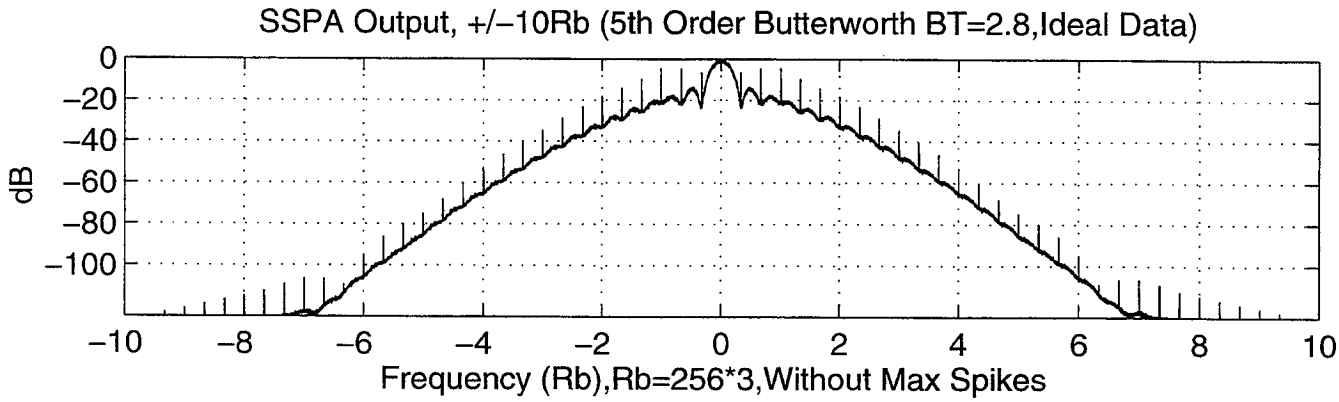

(a)5th Order Butterworth Filter (BT=2.8), $\pm 10R_b$

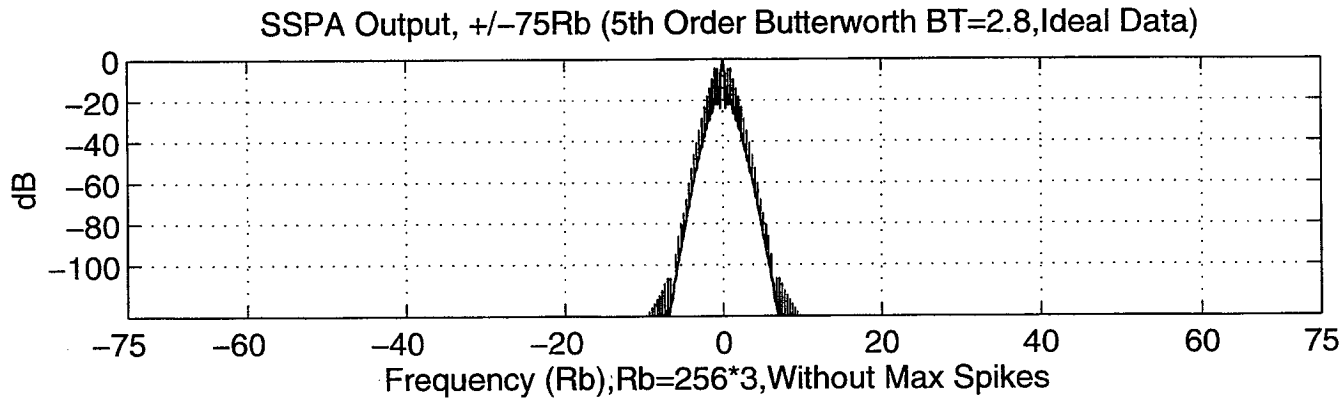

(b)5th Order Butterworth Filter (BT=2.8), $\pm 75R_b$

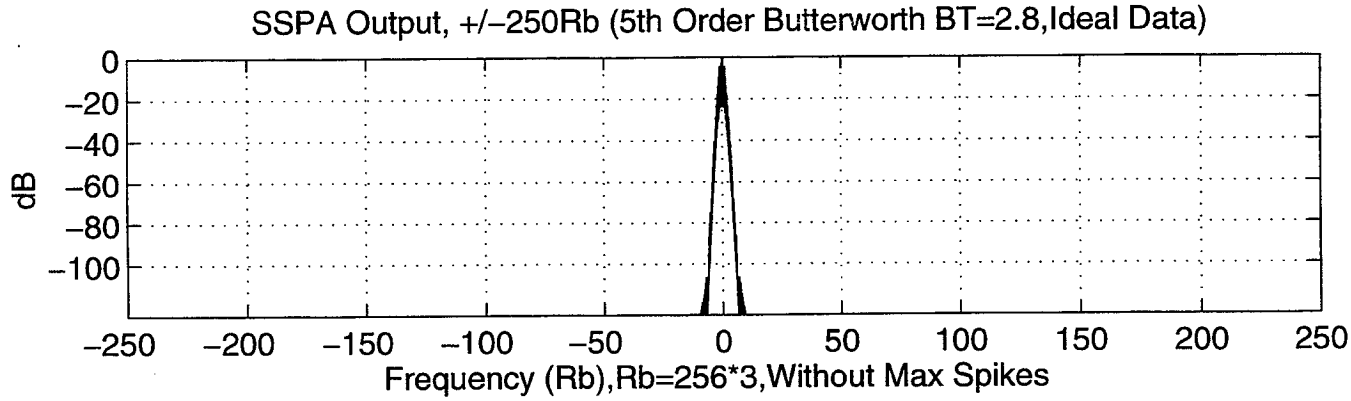

(c) 5th Order Butterworth Filter, BT=2.8, $\pm 250R_b$

Figure 22: 5^{th} Order Butterworth Filter, (BT=2.8) Without Central Spike

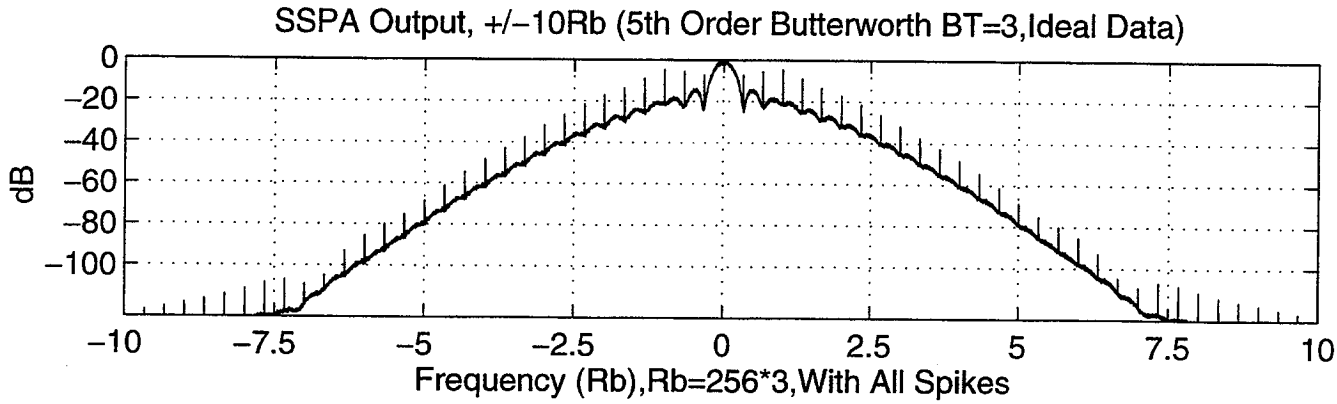

(a) 5th Order Butterworth Filter (BT=3), $\pm 10R_b$

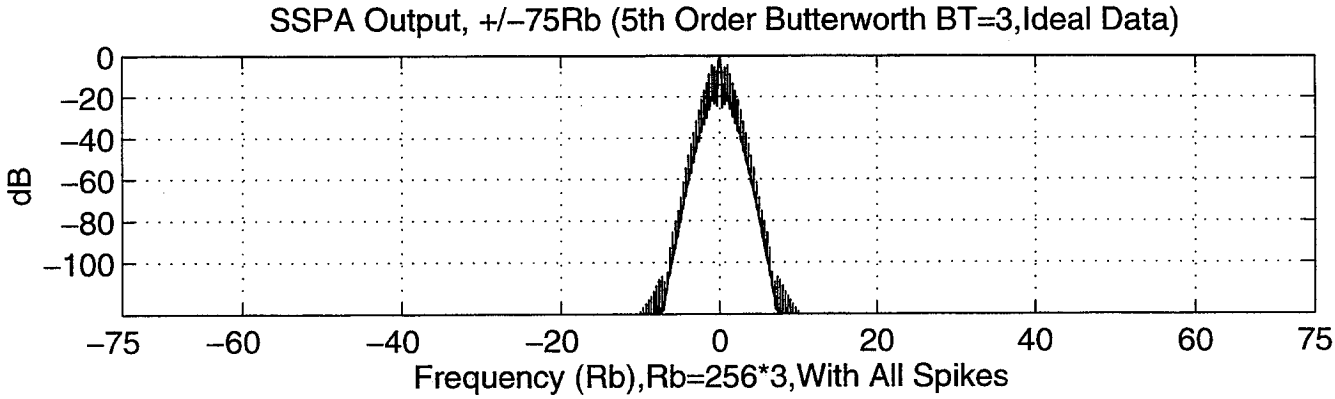

(b) 5th Order Butterworth Filter (BT=3), $\pm 75R_b$

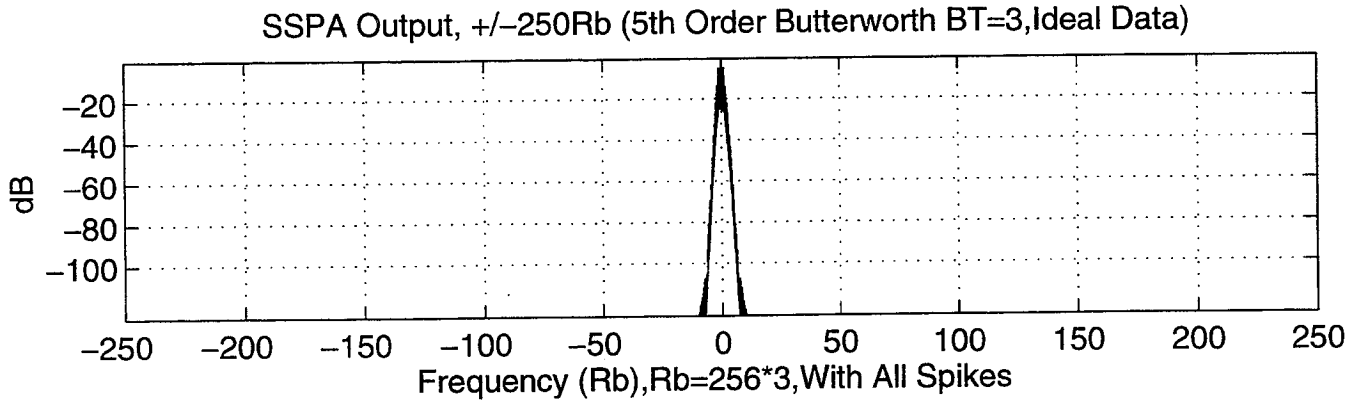

(c) 5th Order Butterworth Filter (BT=3), $\pm 250R_b$

Figure 23: 5^{th} Order Butterworth Filter (BT=3) Power Spectra, With Central Spike

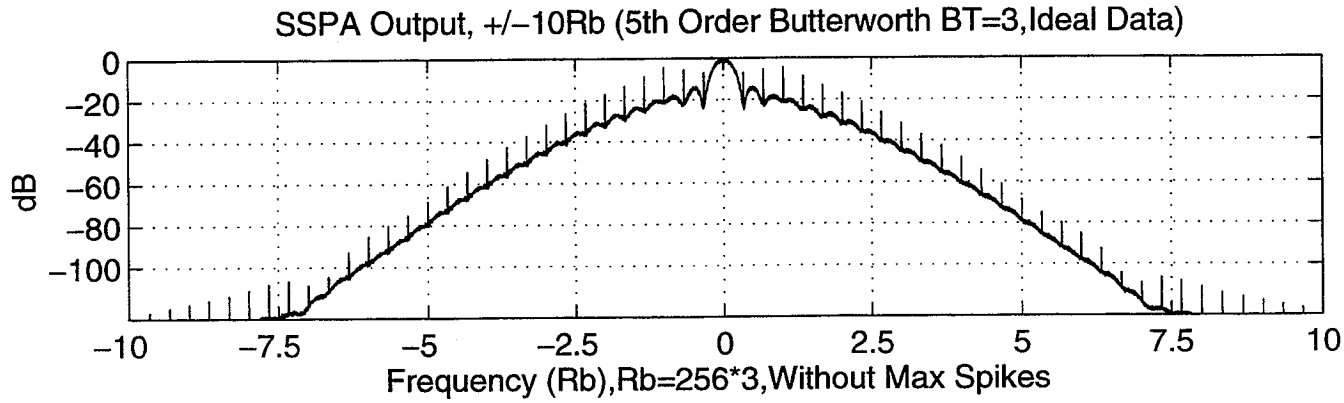

(a) 5th Order Butterworth Filter (BT=3), $\pm 10\ R_b$

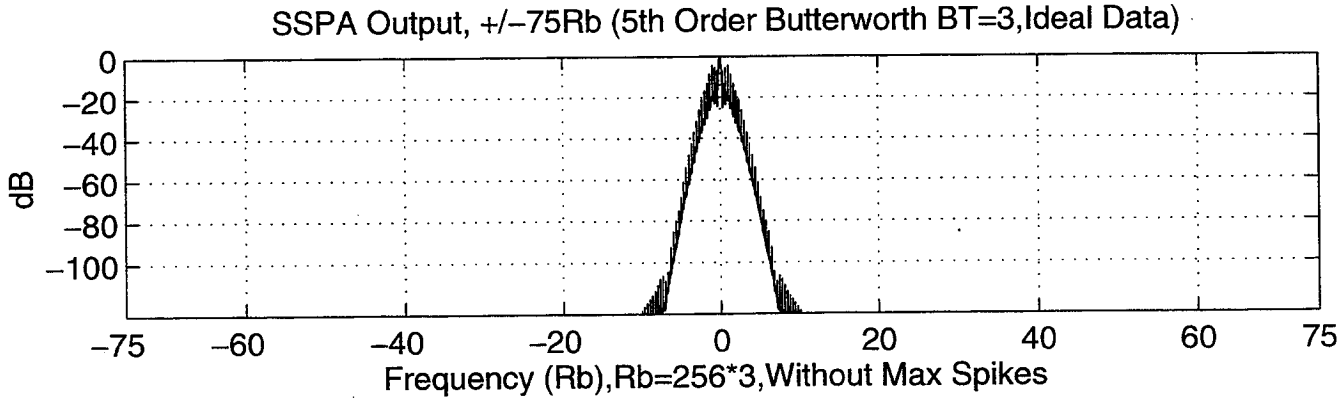

(b) 5th Order Butterworth Filter (BT=3), $\pm 75R_b$

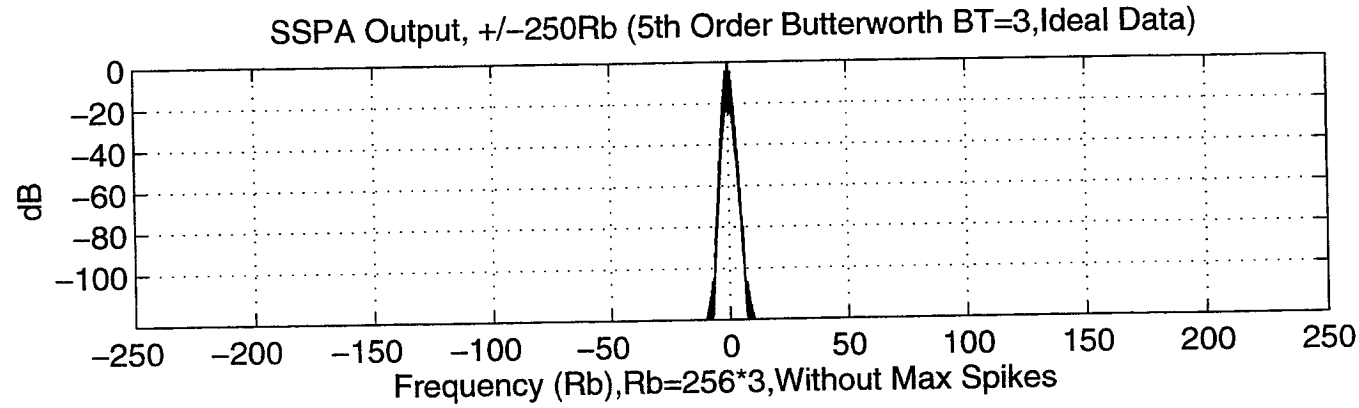

(c) 5th Order Butterworth Filter (BT=3), $\pm 250R_b$

Figure 24: 5^{th} Order Butterworth Filter (BT=3) Without Central Spike

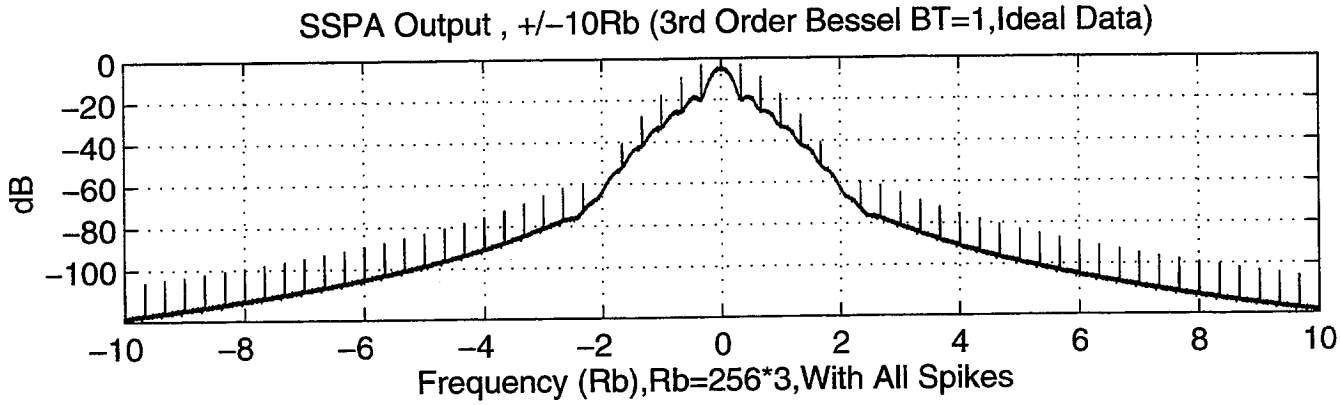

(a) 3rd Order Bessel Filter (BT=1) , $\pm 10R_b$

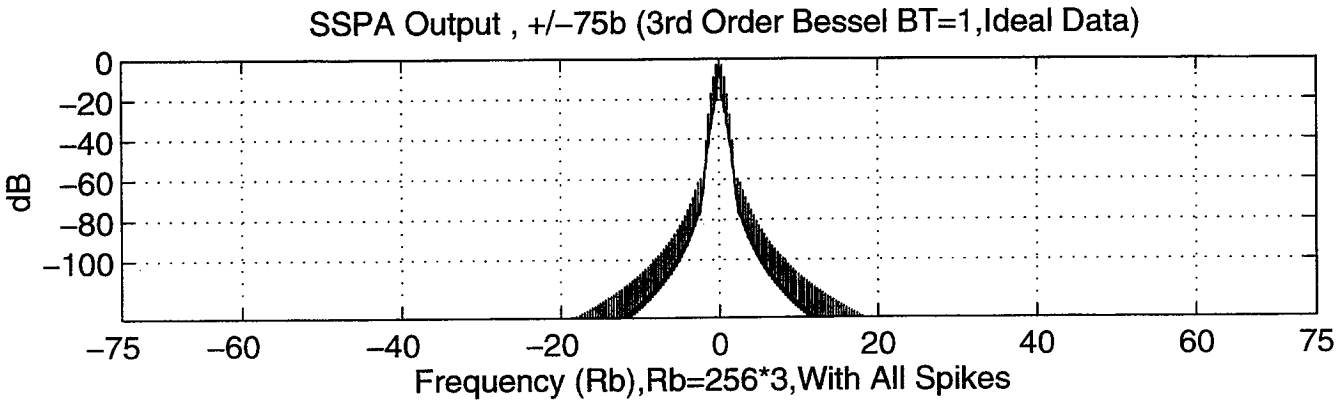

(b) 3rd Order Bessel Filter (BT=1), $\pm 75R_b$

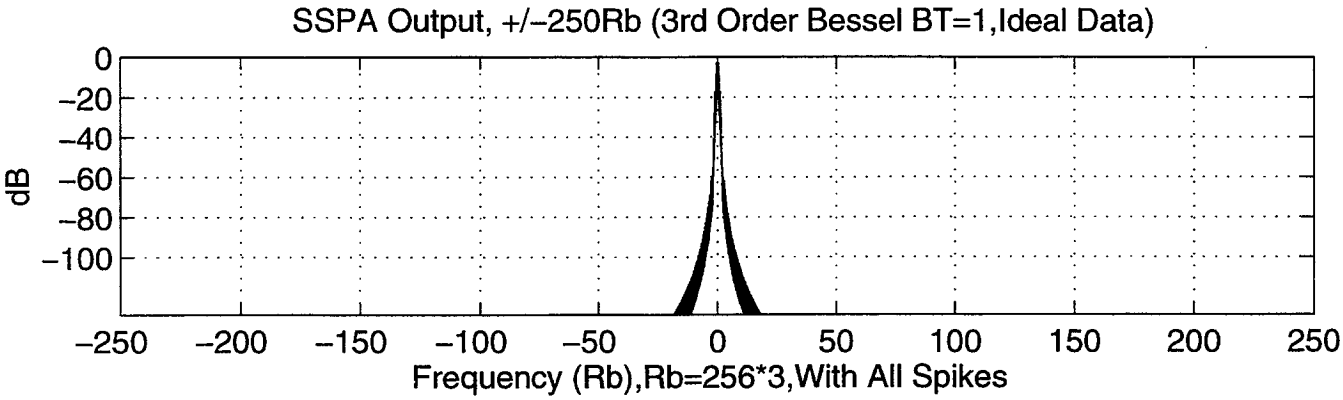

(c) 3rd Order Bessel Filter (BT=1) , $\pm 250R_b$

Figure 25: 3rd Order Bessel (BT=1) Power Spectra, With Central Spike

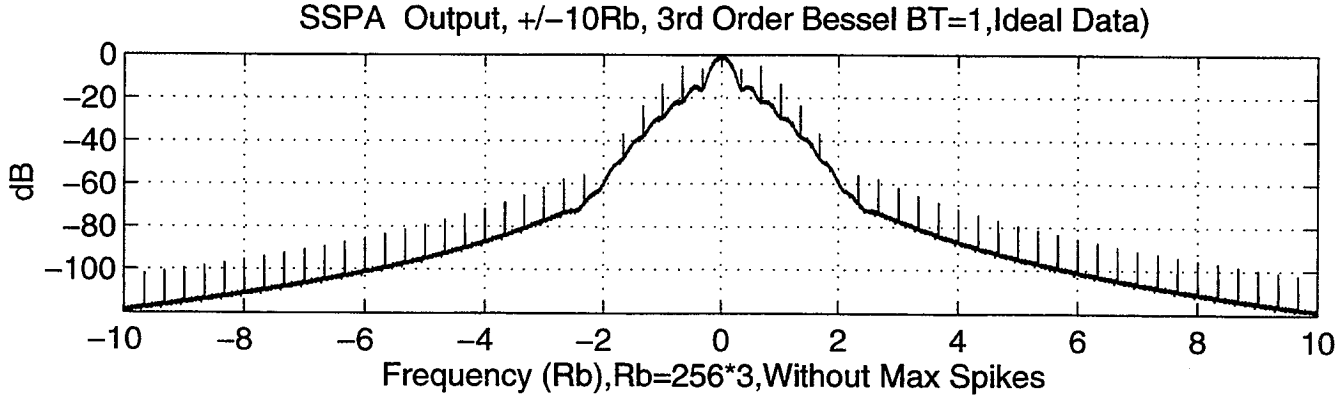

(a) 3rd Order Bessel Filter (BT=1), $\pm 10\ R_b$

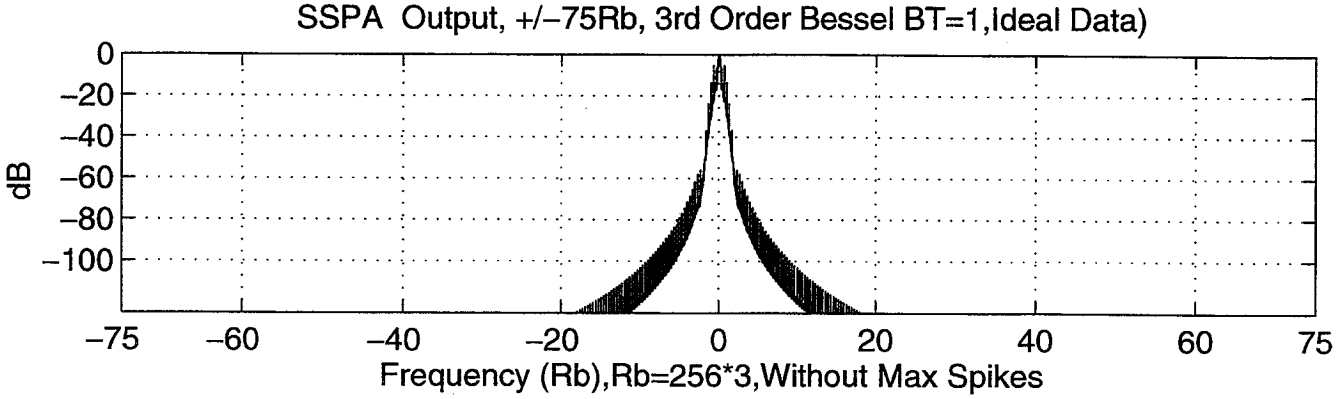

(b) 3rd Order Bessel Filter (BT=1), $\pm 75R_b$

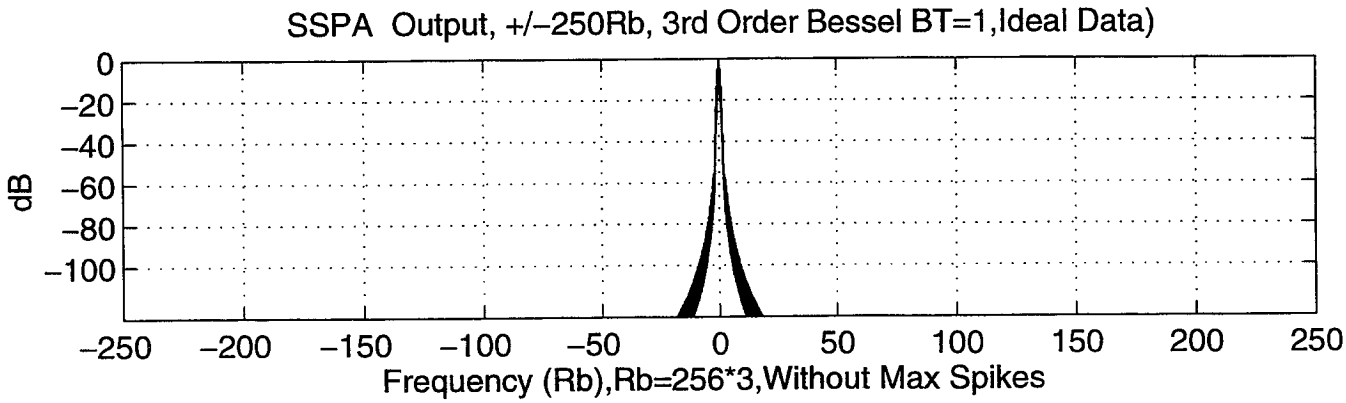

(c) 3rd Order Bessel Filter (BT=1), $\pm 250R_b$

Figure 26: 3rd Order Bessel Filter (BT=1), Without Central Spike

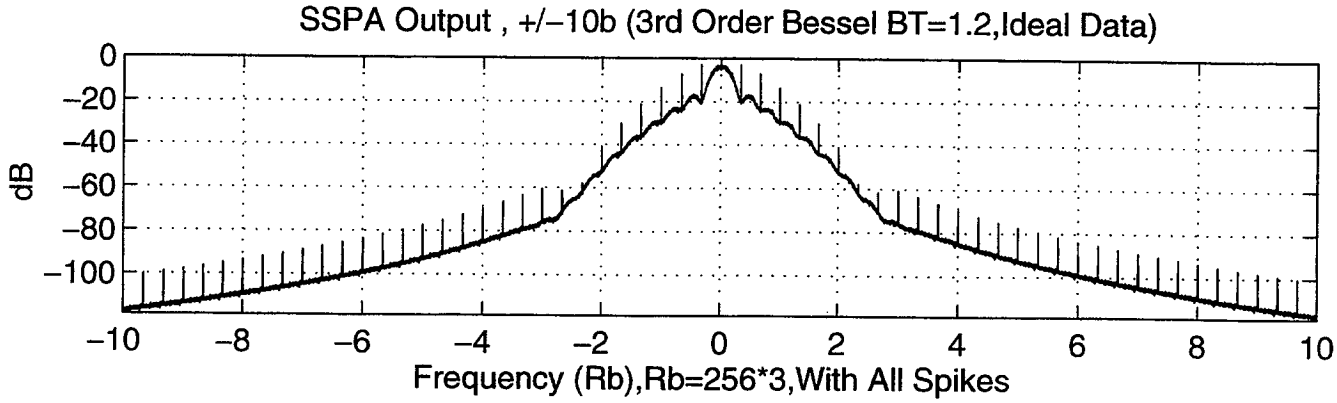

(a) 3rd Order Bessel Filter (BT=1.2), $\pm 10R_b$

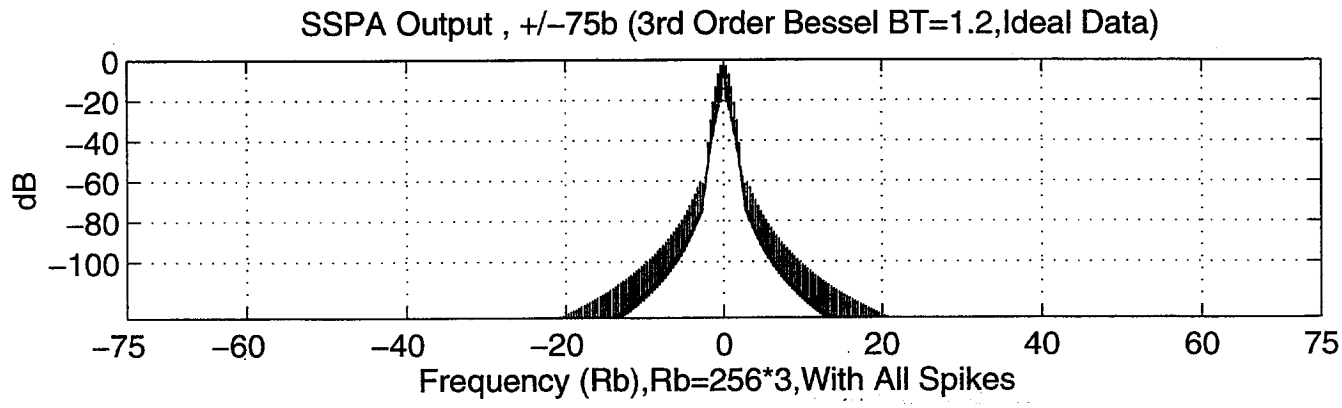

(b) 3rd Order Bessel Filter (BT=1.2) , $\pm 75R_b$

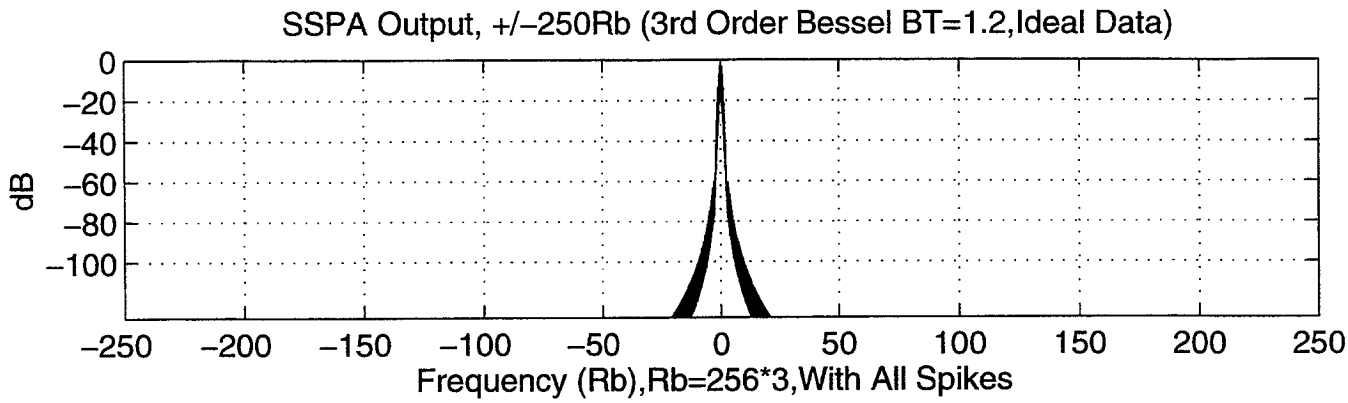

(c) 3rd Order Bessel Filter (BT=1.2), $\pm 250R_b$

Figure 27: 3rd Order Bessel Filter (BT=1.2) With Central Spike

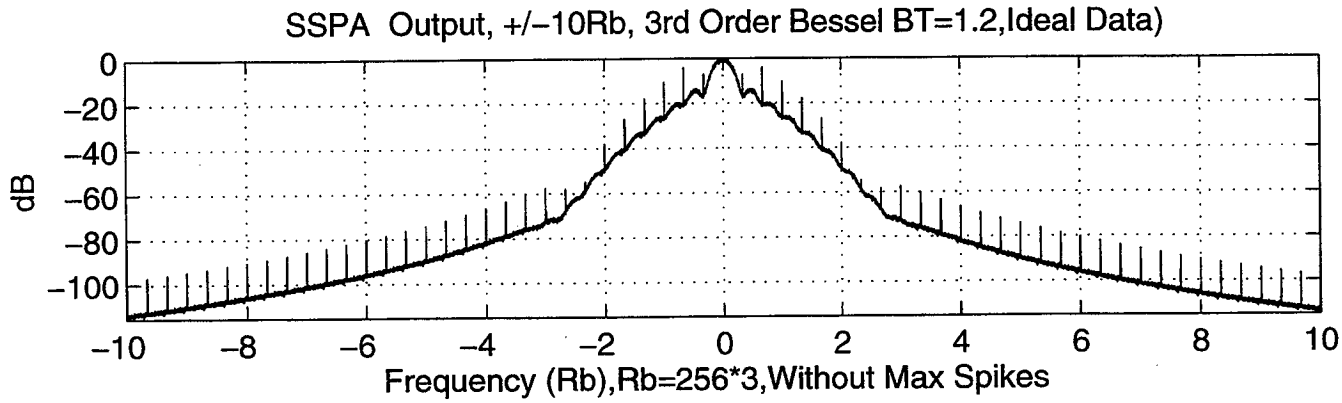

(a) 3rd Order Bessel Filter (BT=1.2), $\pm 10\ R_b$

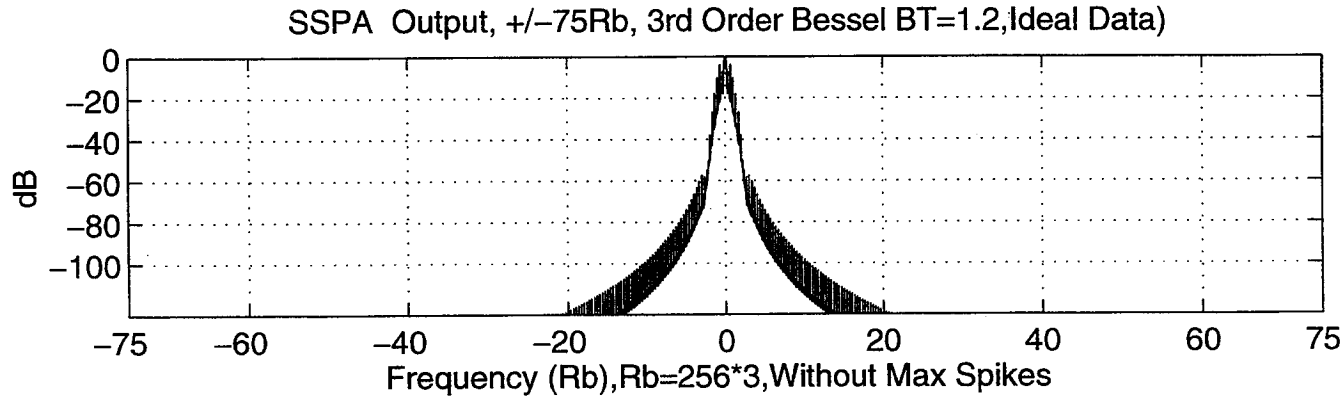

(b) 3rd Order Bessel Filter (BT=1.2), $\pm 75R_b$

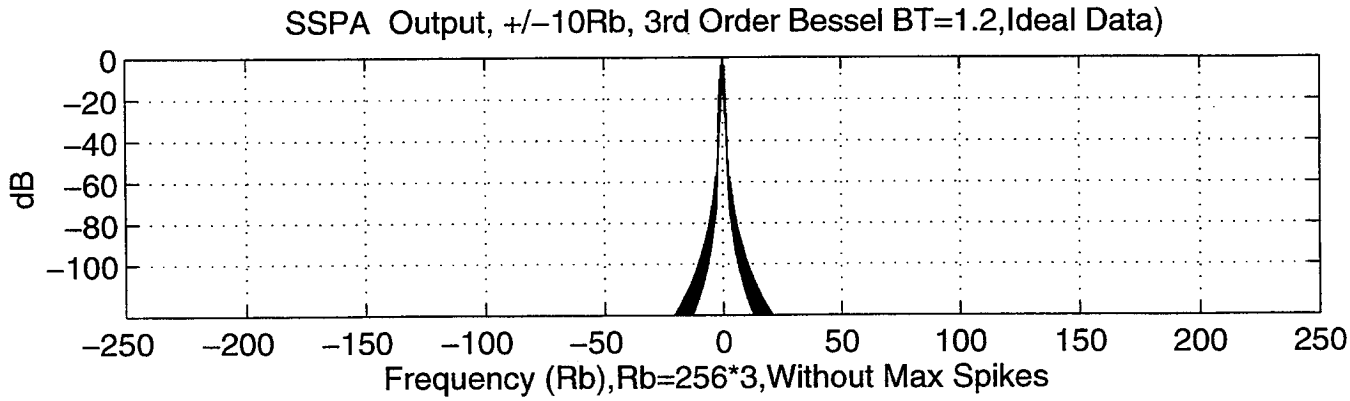

(c) 3rd Order Bessel Filter (BT=1.2), $\pm 250R_b$

Figure 28: 3rd Order Bessel Filter (BT=1.2), Without Central Spike

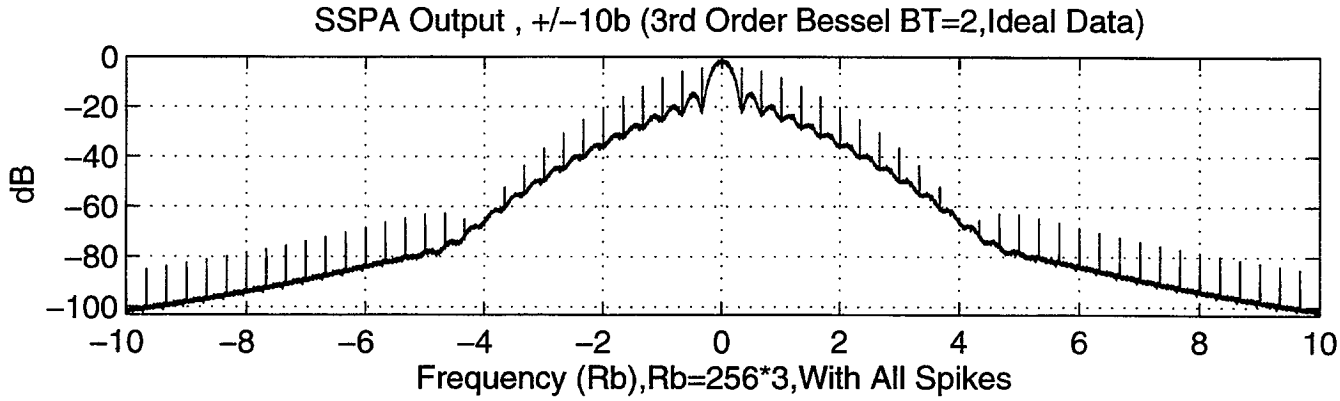

(a) 3rd Order Bessel Filter (BT=2), $\pm 10R_b$

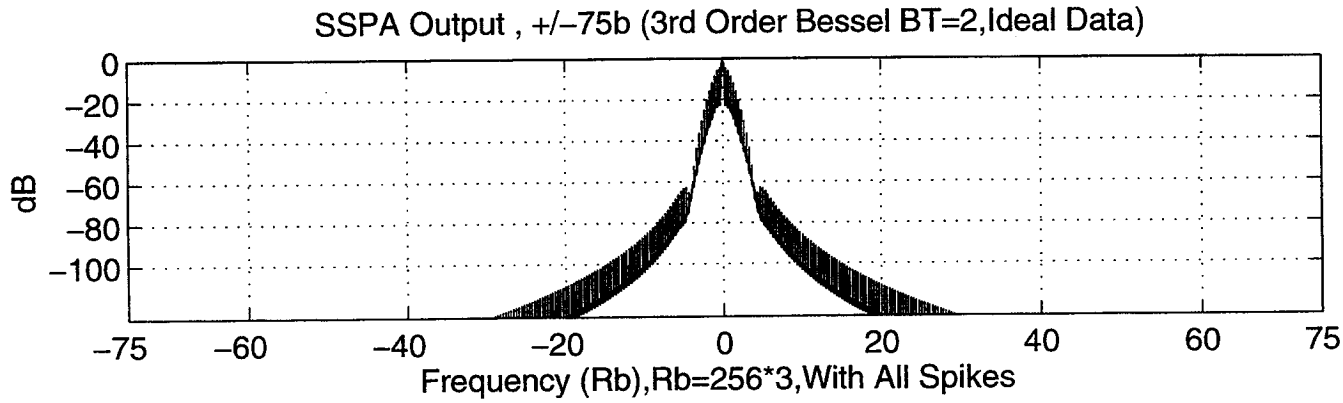

(b) 3rd Order Bessel Filter (BT=2) , $\pm 75R_b$

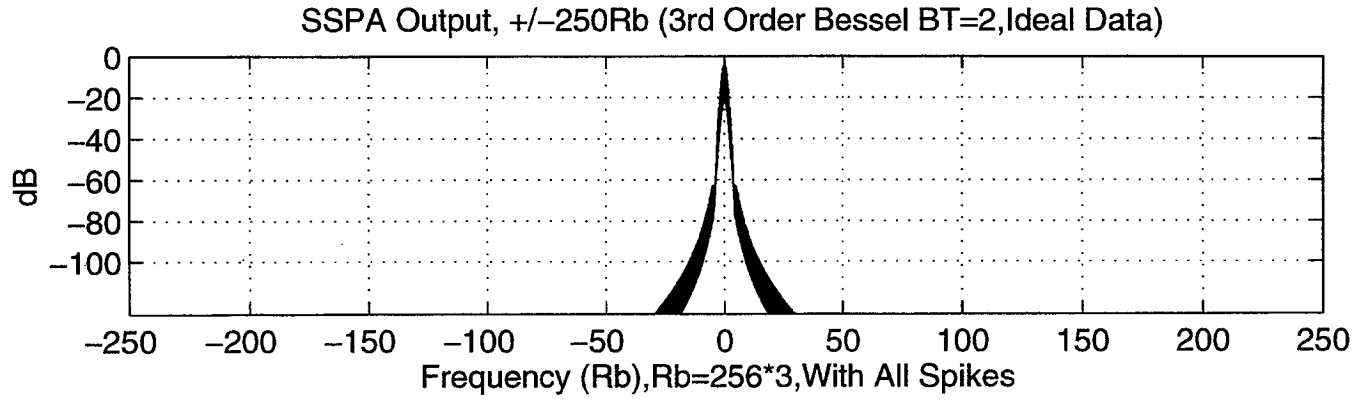

(c) 3rd Order Bessel Filter (BT=2), $\pm 250R_b$

Figure 29: 3rd Order Bessel Filter (BT=2), With Central Spike

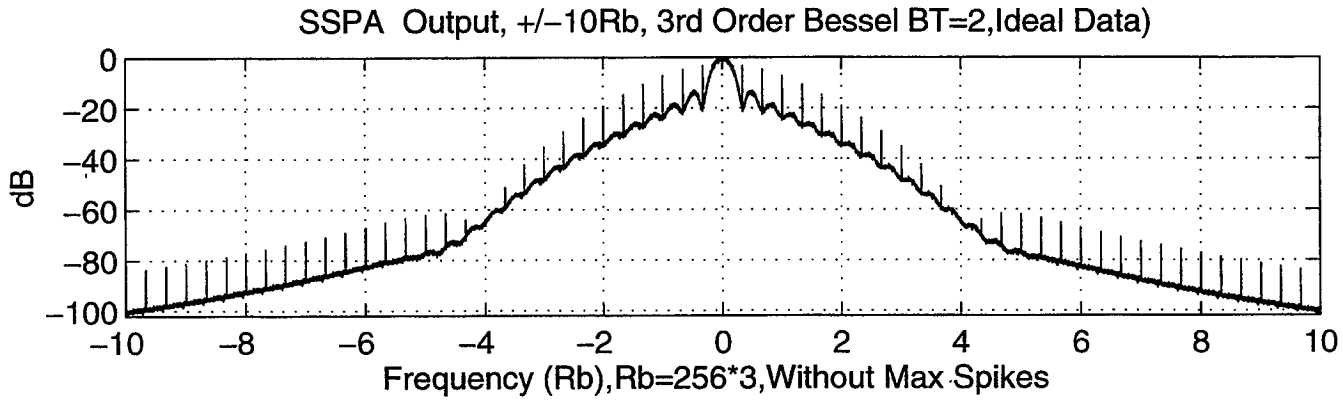

(a) 3rd Order Bessel Filter (BT=2), ± 10 R_b

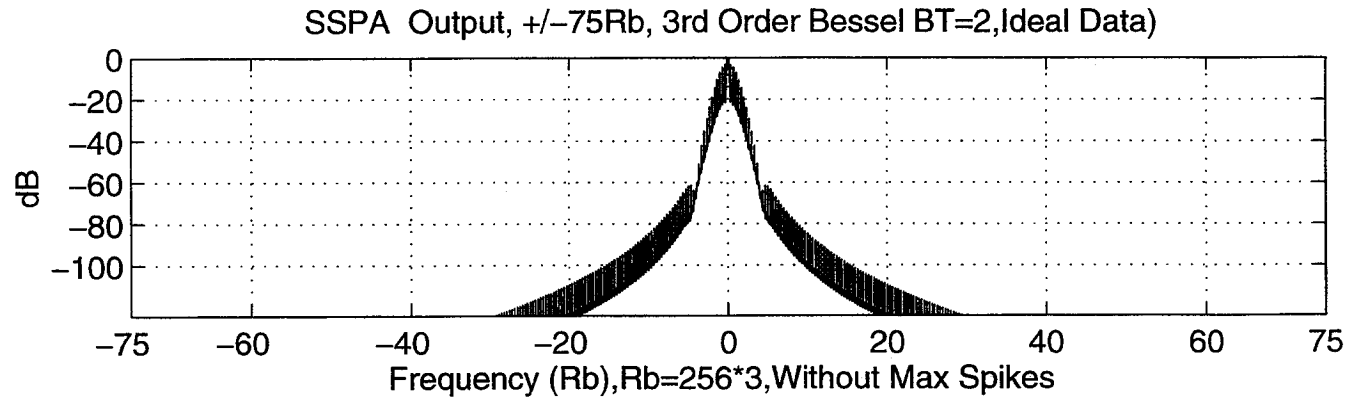

(b) 3rd Order Bessel Filter (BT=2), ± 75R_b

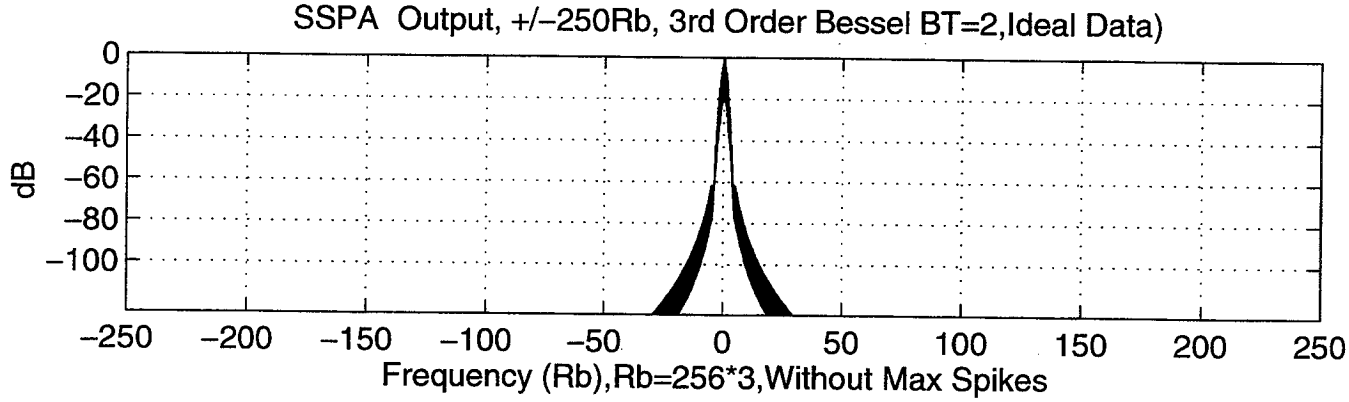

(c) 3rd Order Bessel Filter (BT=2), ± 250R_b

Figure 30: 3rd Order Bessel Filter (BT=2) Without Central Spike

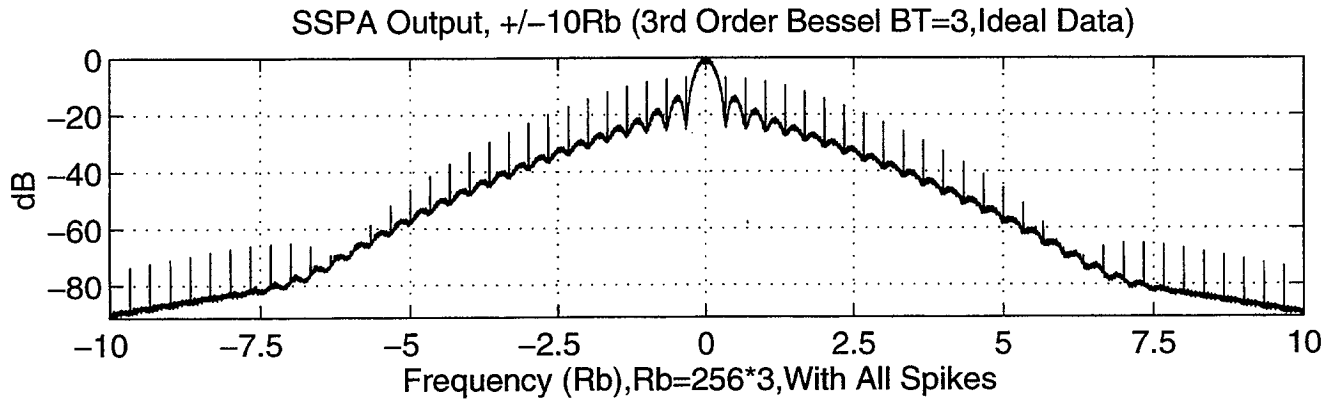

(a) 3rd Order Bessel Filter (BT=3), $\pm 10R_b$

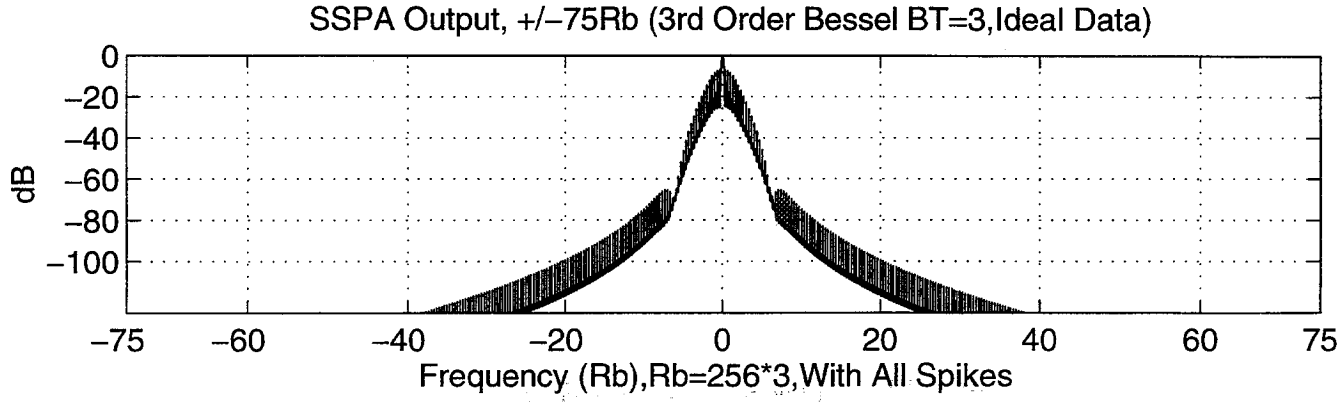

(b) 3rd Order Bessel Filter (BT=3), $\pm 75R_b$

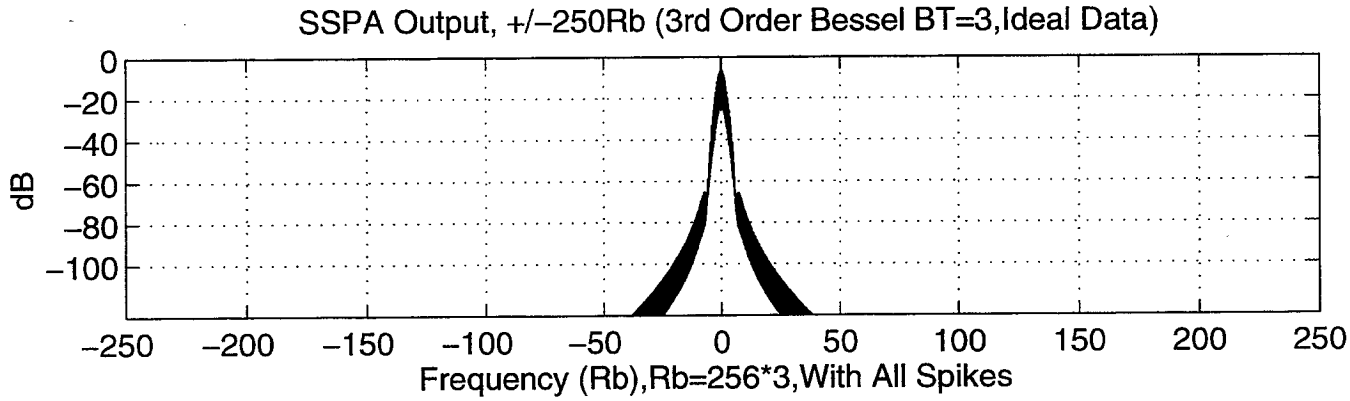

(c) 3rd Order Bessel Filter (BT=3), $\pm 250R_b$

Figure 31: 3rd Order Bessel Filter (BT=3), With Central Spike

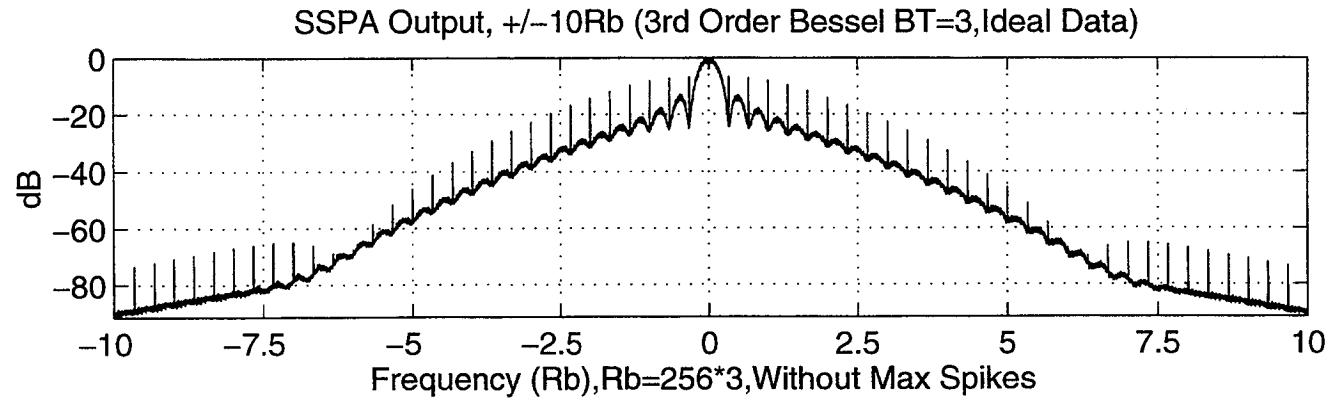

(a) 3rd Order Bessel Filter (BT=3), ± 10 R_b

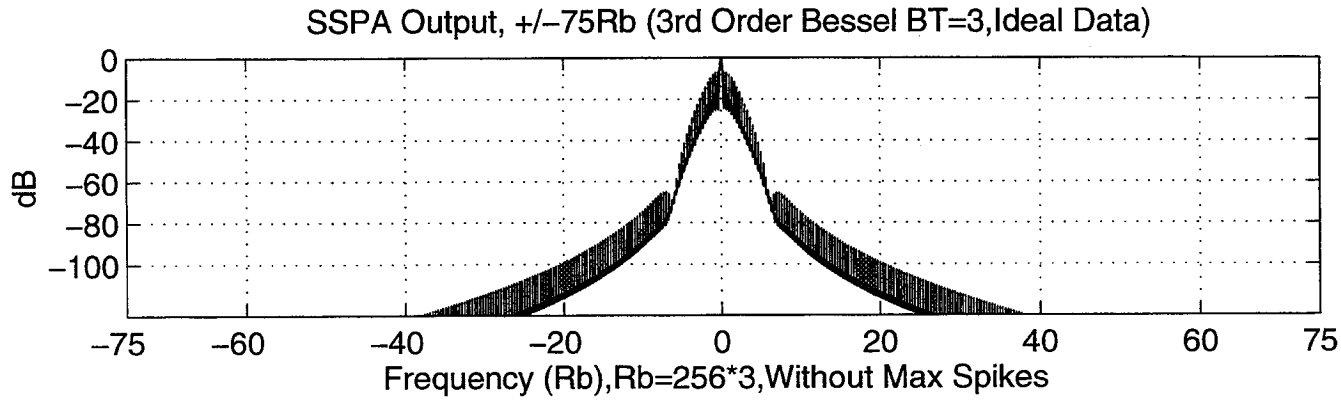

(b) 3rd Order Bessel Filter (BT=3),. ± 75R_b

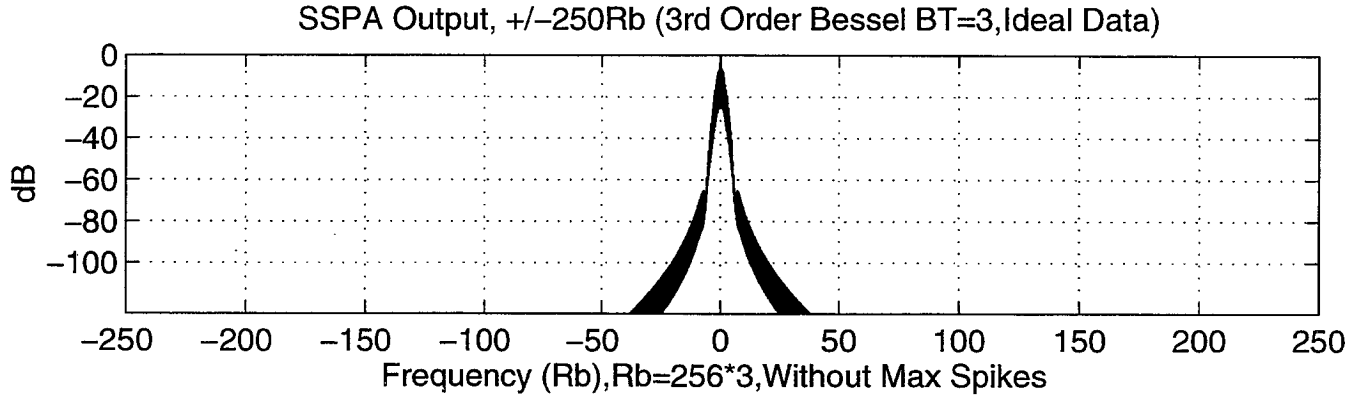

(c) 3rd Order Bessel Filter (BT=3), ± 250R_b

Figure 32: 3rd Order Bessel Filter (BT=3) Without Central Spike

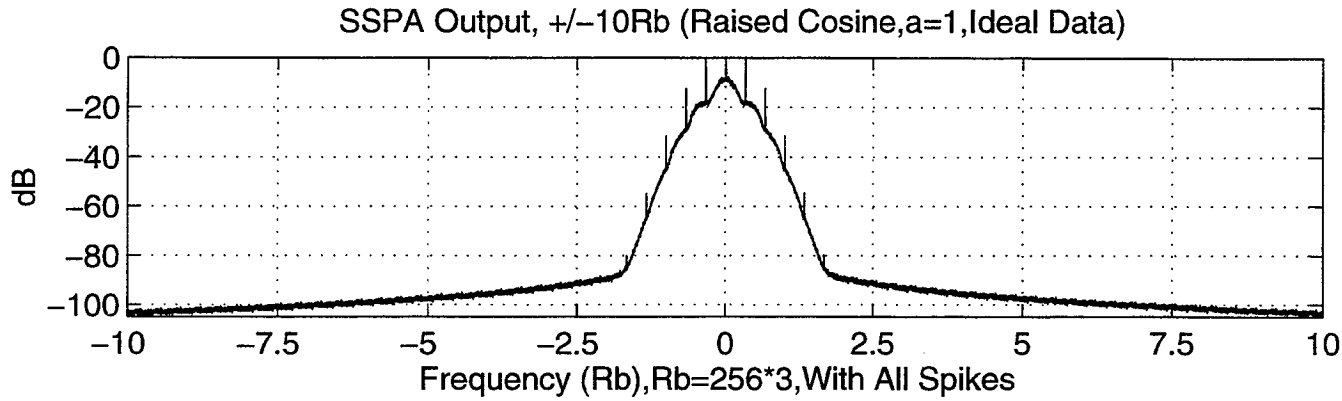

(a) Square-Root Raised Cosine (α =1) , $\pm 10R_b$

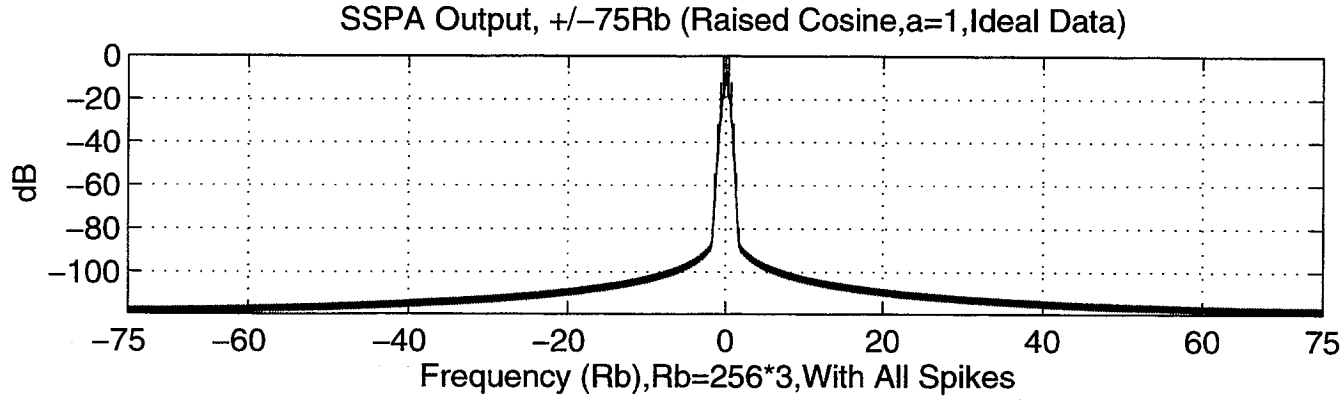

(b) Square-Root Raised Cosine (α =1) , $\pm 75R_b$

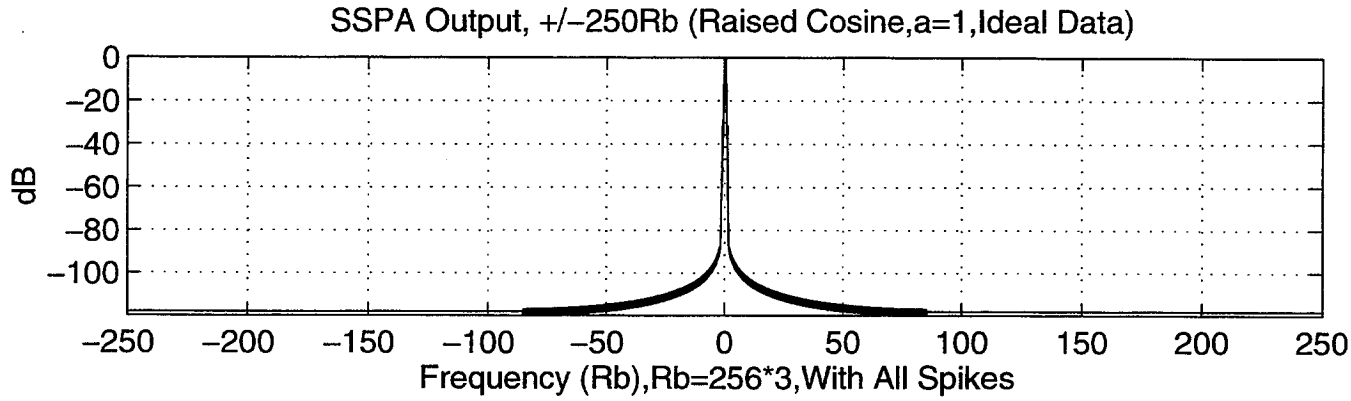

(c) Square-Root Raised Cosine (α =1), $\pm 250R_b$

Figure 33: Square-Root Raised Cosine (α =1) With Central Spike

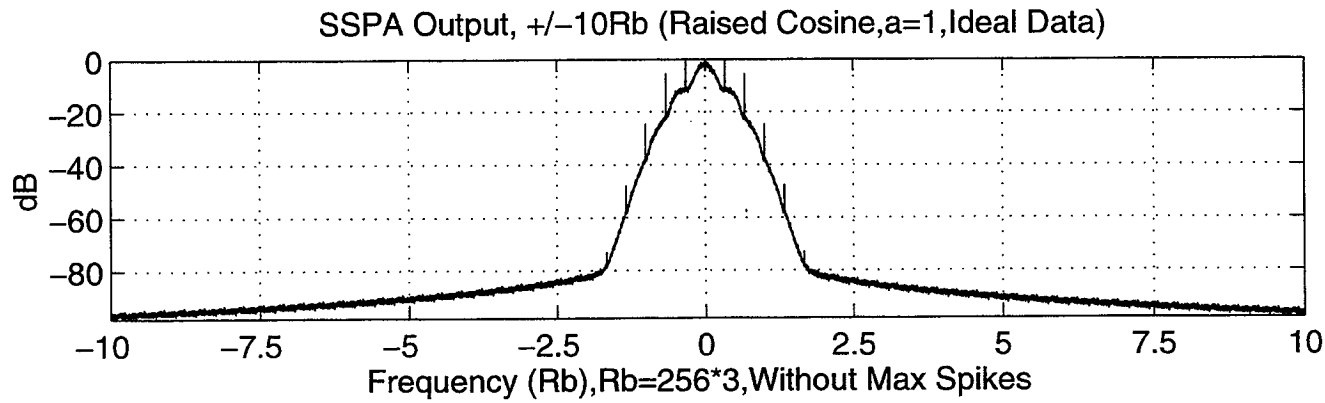

(a) Square-root Raised Cosine (α =1) , $\pm 10\ R_b$

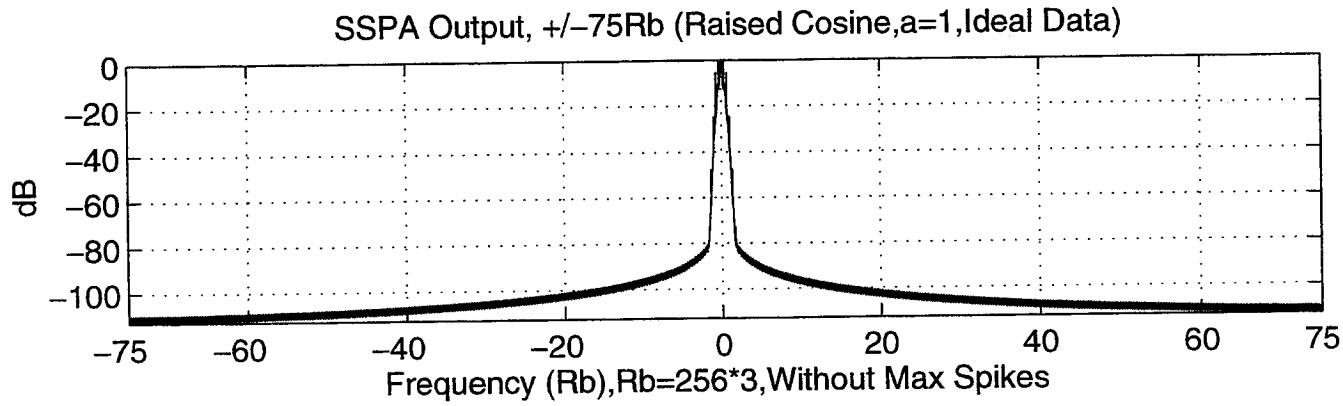

(b) Square-root Raised Cosine (α =1), $\pm 75R_b$

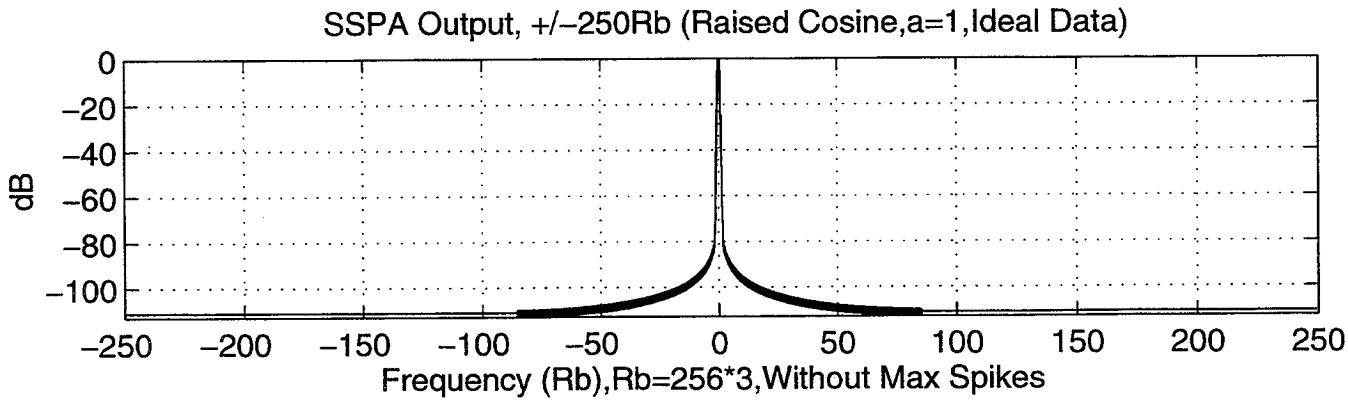

(c) Square-Root Raised Cosine (α =1) , $\pm 250R_b$

Figure 34: Square-Root Raised Cosine (α =1), Without Central Spike

Frequency Band Utilization Ratio(ρ)

The frequency band utilization ratio can be defined as:

$$\rho = \frac{\text{Number of spacecraft with Filtering Accommodated in Frequency Band}}{\text{Number of spacecraft without Filtering Accommodated in Frequency Band}}$$

From the simulations, the utilization ratios (type B) were calculated and listed in Table 2 along with the utilization ratios for Type A[5]. From the utilization ratio table, for the same BT and baseband filters, modulator type B has a higher frequency band utilization ratio than type A.

Utilization Ratio (Type A)

Filter Type	-50 dB point	utilization
None	35Rb	1
Butterworth(5th order)BT=1	2.5Rb	14
Beset (3rd order) BT=1	2.95Rb	11.86
SRRC rolloff=1	2.5Rb	14

Utilization Ratio (Type B)

Filter Type	-50 dB point		utilization	
	with spikes (R_b)	no spikes (R_b)	with spikes	no spikes
None	35		1	1
Butterworth(5th order) BT=1	1.22	1.28	28.7	27
Butterworth(5th order) BT=2	2.38	2.43	14.7	14.4
Butterworth (5th order) BT=2.8	3.2	3.23	11	10.8
Butterworth (5th order) BT=3	3.45	3.45	10.1	10.1
Beset (3rd order) BT=1	1.625	1.75	21.5	20
Beset (3rd order) BT=1.2	1.88	2.04	18.6	17.1
Beset (3rd order) BT=2	3.1	3.22	11.3	10.8
Beset (3rd order) BT=3	4.5	4.53	7.8	7.7
SRRC rolloff=1	1.11	1.23	31.5	28.5

Table 2 Utilization Ratio of Type A and B 8 PSK

Bit Errors Rates Simulations

The bit errors are produced due to the ISI and AWGN. This report provides the measure of bit errors according to bit energy to noise ratio(Eb/N_o).Figure 15 shows the system block diagram for measuring bit error rates. For different filter types and their positions(type A or B), the BERs are put together for comparison. The BER plots are given in Figure 35-40.

The following parameters were used to obtain the bit error rates:

Data source:

a. Ideal data with p(0)(probability of zero)=0.5;
b. Sample Rate (f_s) = 16 Hz
c. Symbol rate R_s=1 (Bit rate=3; 16 samples/symbol);

Base band Filters

a. Butterworth 5th Order (BT=1,2,2.8,3)
b. Bessel 3rd Order (BT=1,1.2,2,3)
c.SRRC(α =1,Number of tap length=16*16=256, rectangular window, Square-root raised cosine='yes'; Sample input='yes')

Power Amplifier:

European Space Agency(ESA) 10-watt SSPA , Back off =0dB as obtained from JPL

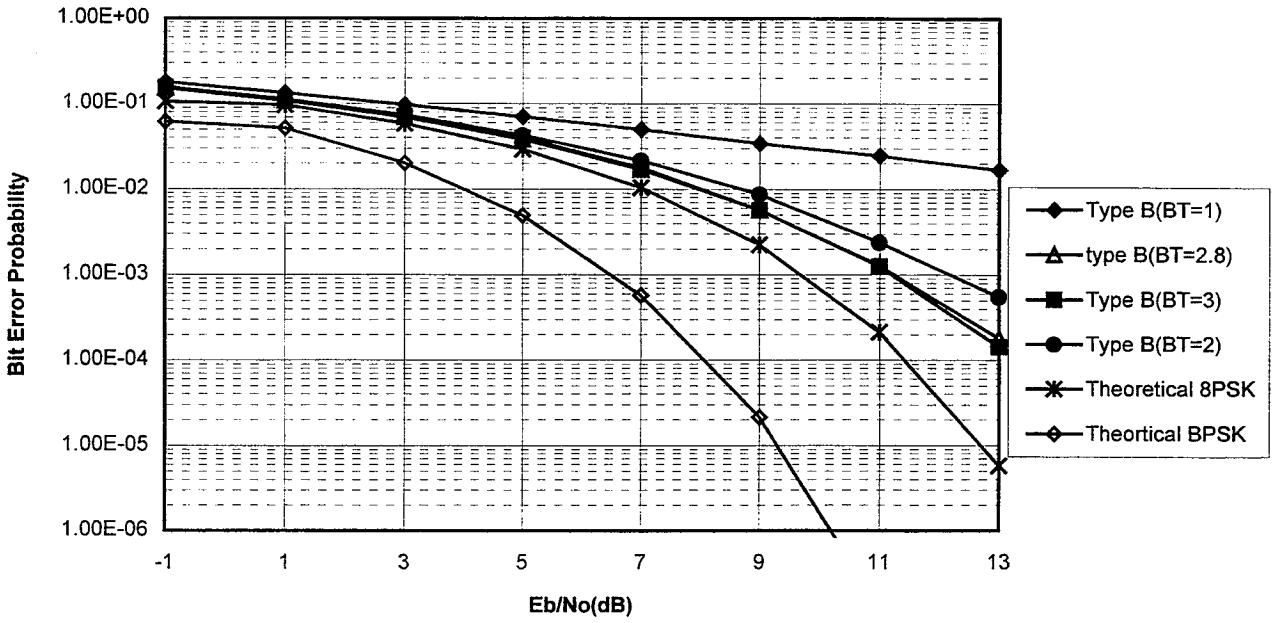

Figure 35. BER Plot For 5th Order Butterworth Filters(Type B)

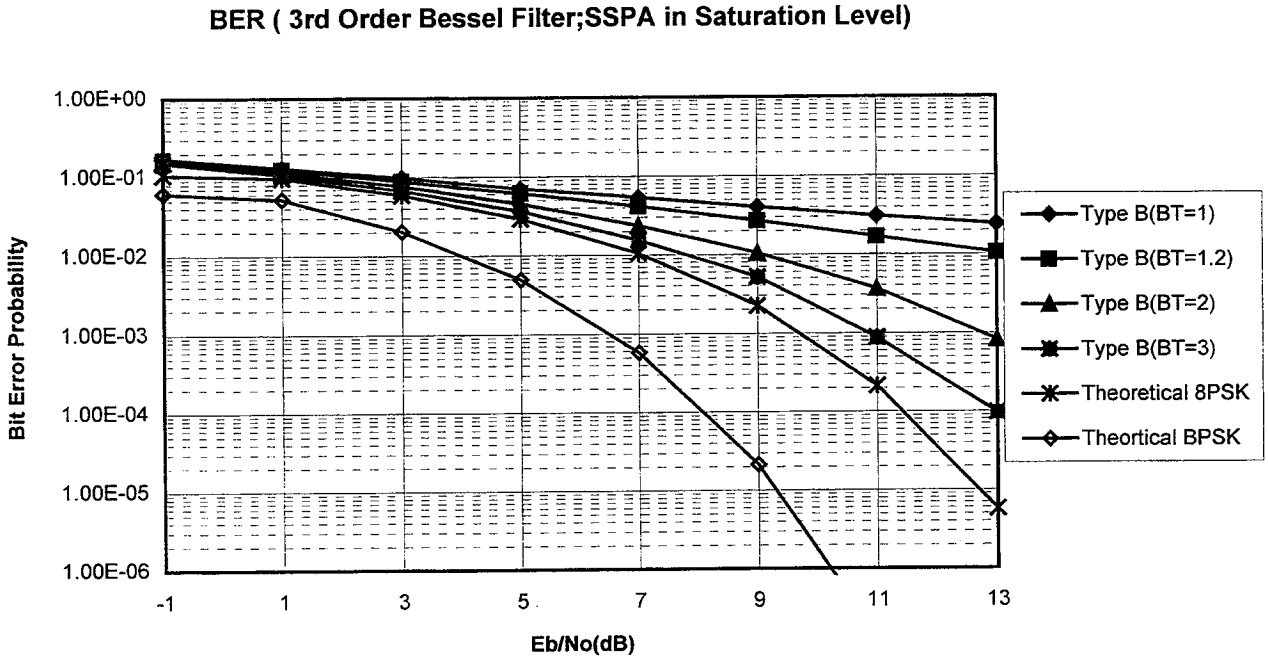

Figure 36 BER For 3rd Order Bessel Filters (Type B)

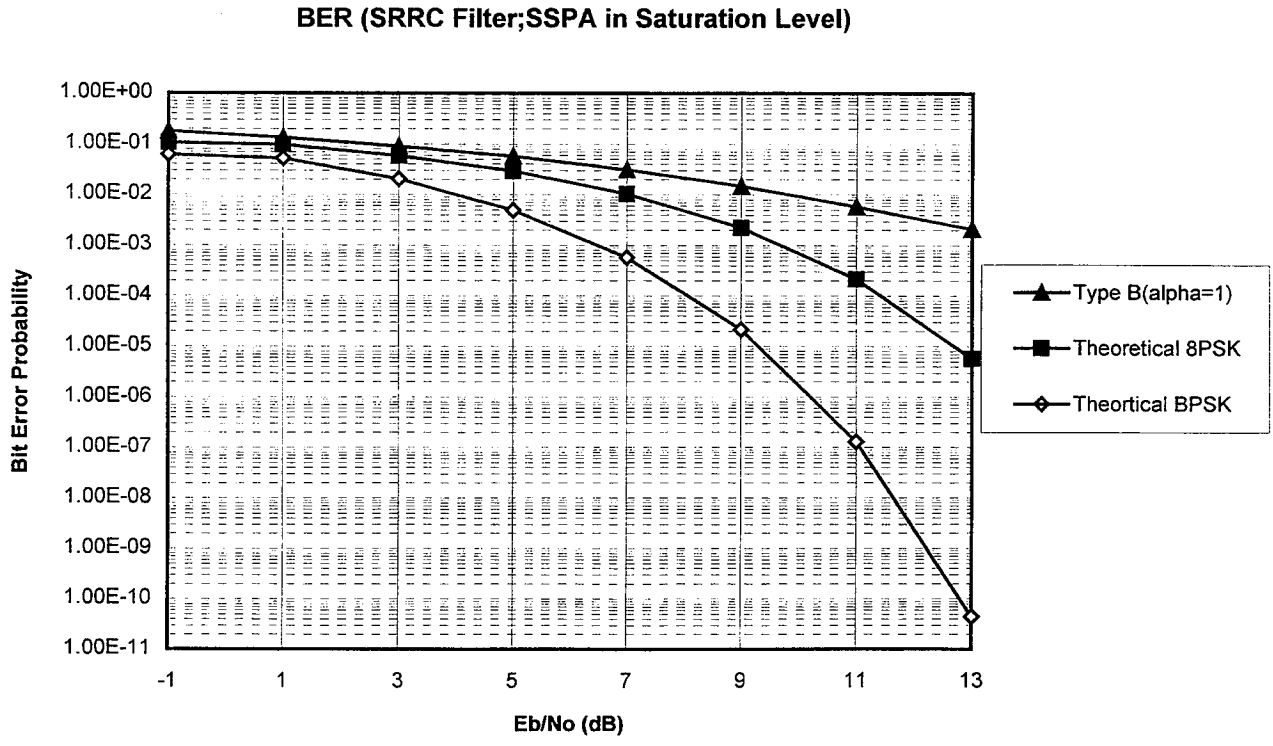

Figure 37 BER Plots For SRRC Filters (Type B)

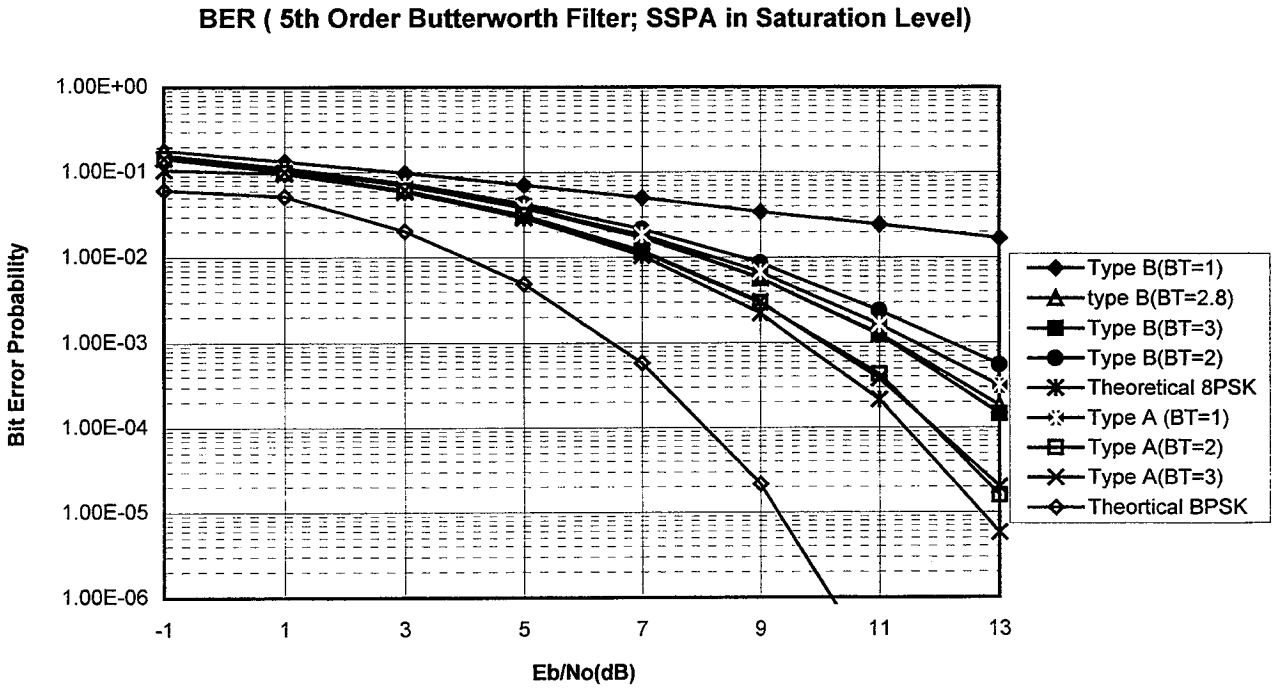

Figure 38. BER Plot For 5th Order Butterworth Filters(Type A And B)

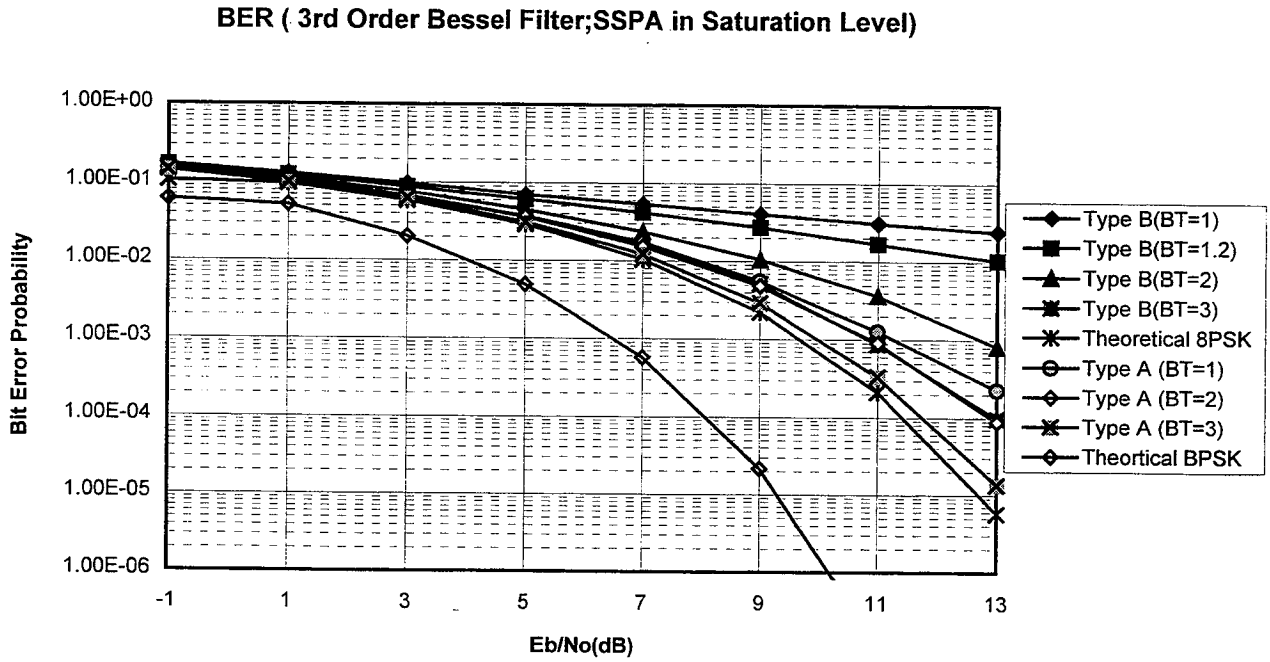

Figure 39 BER For 3rd Order Bessel Filters (Type A And B)

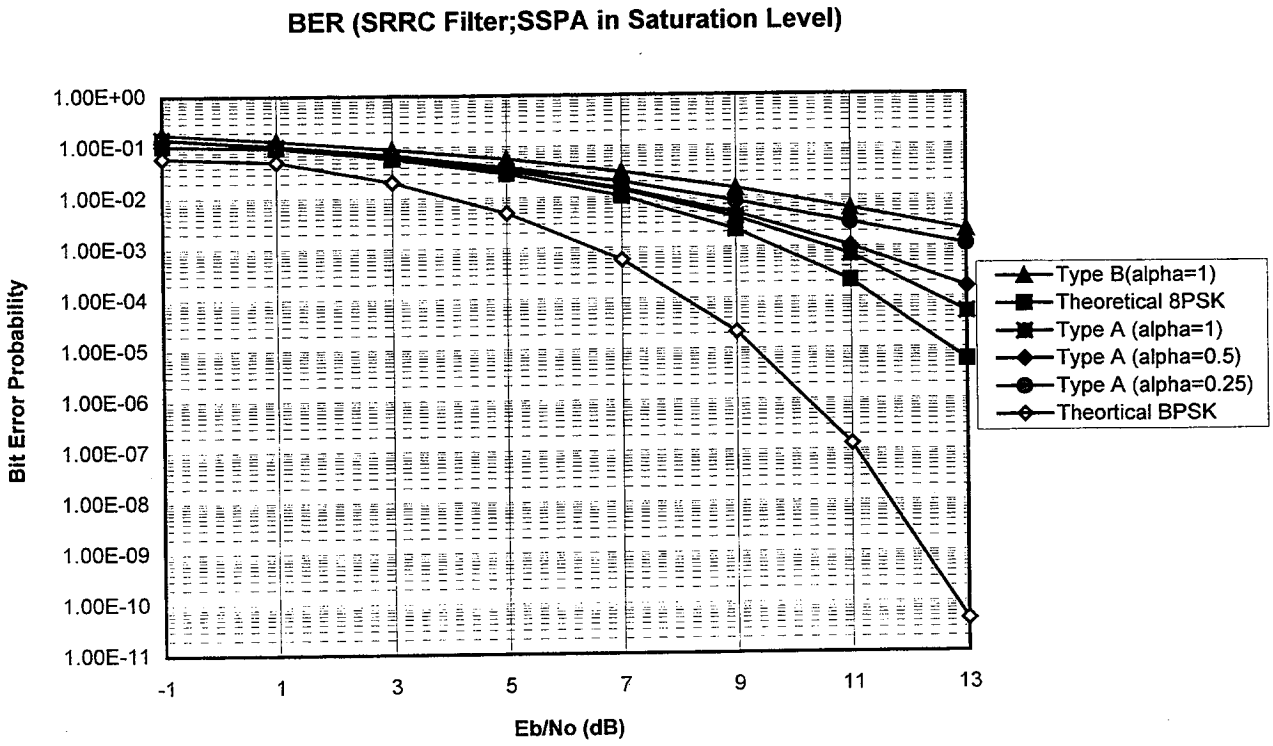

Figure 40 BER Plots For SRRC Filters (Type A And B)

ISI Losses Due To Filter

The ISI losses due to the pulse shaping filter can be determined by the BER simulations. The following tables gives the results of baseband filter ISI losses at 10^{-3} BER compared to theoretical 8 PSK(or BPSK) and the filtered 8 PSK.

Filter Type	Loss BT=1 (dB)	Loss BT=1.2 (dB)	Loss BT=2 (dB)	Loss BT=2.8 (dB)	Loss BT=3 (dB)
Butterworth 5th Order	22.5-10= 12.5	----------	12.32-10= 2.32	11.48-10= 1.48	11.48-10= 1.48
Bessel 3rd Order	----------	20-10= 10	12.85-10= 2.85	----------	11.20-10= 1.20
SRRC(α=1)	14.22-10= 4.22	----------	----------	----------	----------

Table 3 Baseband Filters ISI Loss Measurements at 10^{-3} BER(Compared to ideal 8PSK)

Filter Type	Loss BT=1 (dB)	Loss BT=1.2 (dB)	Loss BT=2 (dB)	Loss BT=2.8 (dB)	Loss BT=3 (dB)
Butterworth 5th Order	22.5-6.8= 15.7	----------	12.32-6.8= 5.52	11.48-6.8= 4.68	11.48-6.8= 4.68
Bessel 3rd Order	----------	20-6.8= 13.2	12.85-6.8= 6.05	----------	11.20-6.8= 4.88
SRRC(α=1)	14.22-6.8= 7.42	----------	----------	----------	----------

Table 4 Baseband Filters ISI Loss Measurements at 10^{-3} BER(Compared to ideal BPSK)
(dashes indicate that the simulation was not performed)

As stipulated in [9], the optimum filter should have the smallest BT value and provide losses<0.4 dB. Thus a higher order of BT should be simulated to find an optimum BT and meet the requirement of ISI loss <0.4. The Figure 41 shows the relationship of ISI loss and utilization ratio for different filters.

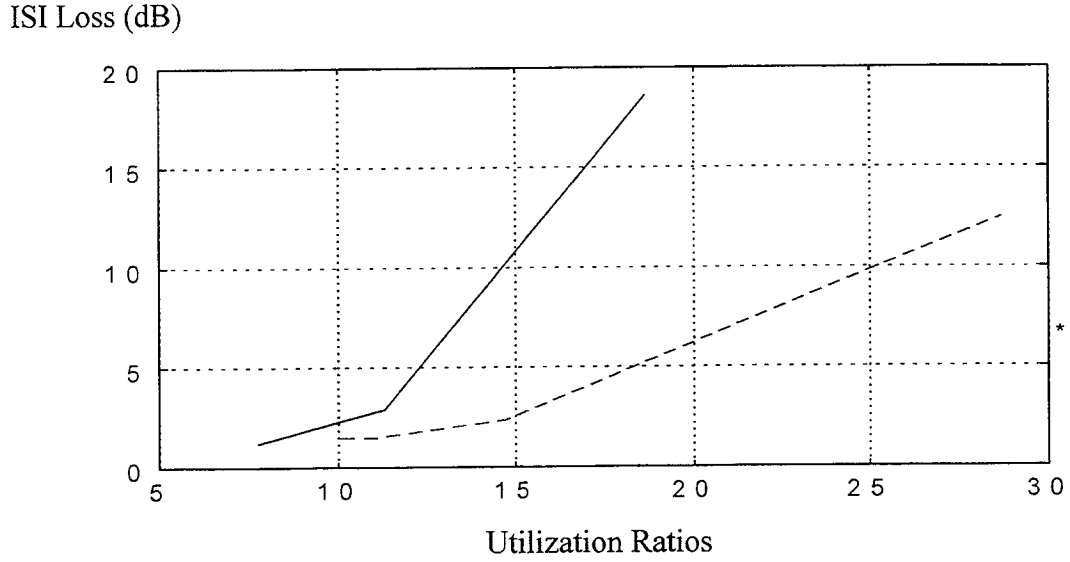

Figure 41. Plots For ISI Loss As Utilization Ratios (Type B)
(------ for 5th Order Butterworth Filter ; ..... for 3rd Order Bessel Filter; * for SRRC filter)

CONCLUSIONS AND SUGGESTIONS

The simulations conducted in the Space Communication and Telemetry Laboratory at NMSU on the pulse shaped 8 PSK modulations were concluded as follows.

Different types and positions of baseband filters have different effects for narrowing bandwidth or frequency band utilization ratio. In general, type B had better results for narrowing the bandwidth than type A did for the same BT value.

Different types and positions of baseband filters also have different effects on producing bit error rates. In general, type A had lower bit error rates than type B. In general, that means that the narrower the bandwidth ,the larger the bit error rate. For the 3rd Order Bessel filter, the BER produced by type A(BT=2) is almost the same as that produced by type B (BT=3). For the 5th Order Butterworth filters, the BER produced by type B(BT=2.8 or 3) is between those produced by type A (BT=1) and type A(BT=2).

A matched filter is crucial for receiving the signal to lower the BER. Integrate and dump circuits can exactly match pulse signals, but for pulse shaped signals it could not match perfectly. A new matched filter which can match pulse shaped signals is needed so that the BER can be reduced further. More filter types and larger BT(BT>4) should be simulated to find an optimal filter and BT. The Spikes that are prevalent in the power spectra should be investigated and ways to reduce or eliminate them should be found.

Work has been performed with 8 PSK (with no pulse-shaping) passed through a non-linear satellite channel consisting of a prefilter, Traveling Wave Tube Amplifier, (TWTA), and a post filter [14]. The pre and post filters were 6^{th} order Butterworth filters with a BT=0.75. Equalizer methods were investigated to counter the nonlinear ISI created by the system. These equalizer techniques included a fixed Volterra Equalizer adapted with an Least Mean Square (LMS) algorithm, an Adaptive Fractionally-Spaced Equalizer (FSE) with the Volterra Equalizer, a Single Filter (SF) Maximum-Liklihood Sequence Detector (MLSD), and a matched filter bank MLSD (MFB-MLSD). These same techniques could be used to counter the non-linear ISI created by the pulse shaping and therefore decrease the BER. A block diagram of the system and some of the results from [14] are given in Figure 42, however for a detailed description see [14].

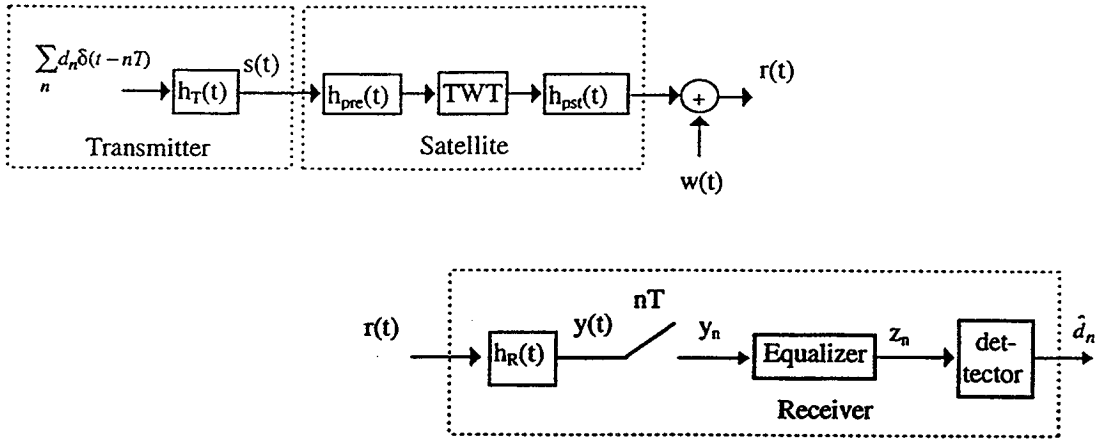

(a) Communication System Model Used for Equalization

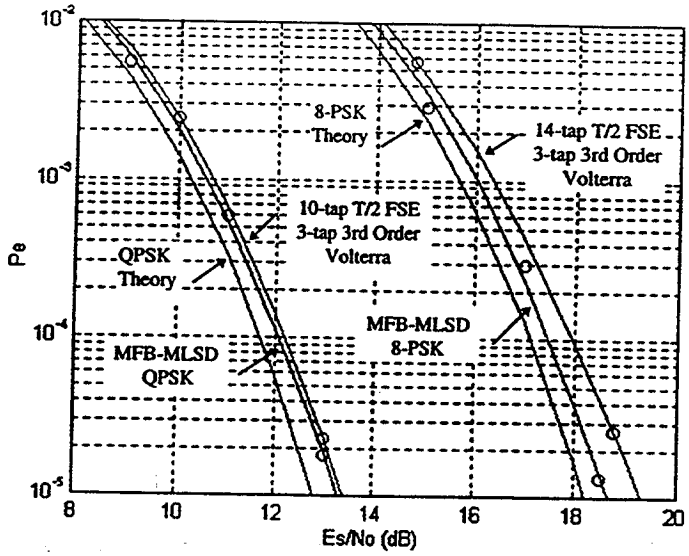

(b) Performance of MFB-MLSD receiver compared to FSE-Volterra receiver

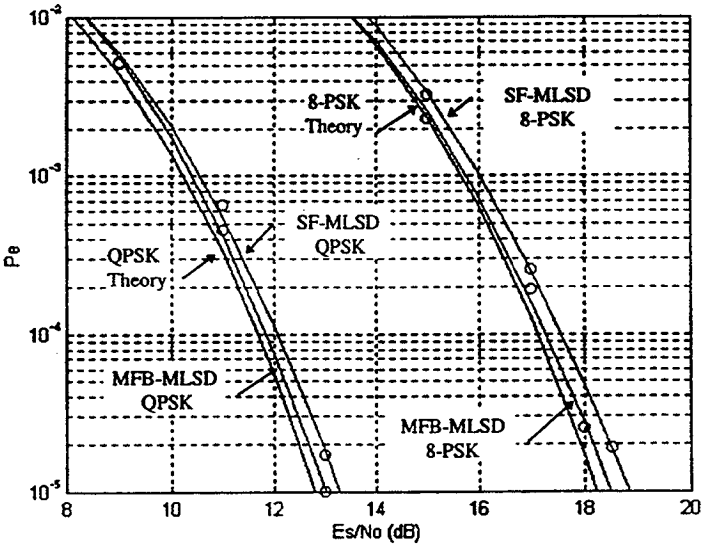

(c) Performance of SF-MLSD and MFB-MLSD receivers

Figure 42: Some Results of Simulations Using Equalizers

REFERENCE

[1] "SPW - The DSP Framework Communications Library Reference," by Comdisco Systems, Product Number: SPW8015, March 1994.

[2] "Signal Processing WorkSystem DSP Library Reference," by Alta Group of Cadence Design Systems, Inc. Product Number: SPW8015, March 1995.

[3] "Signal Processing WorkSystem Interactive Simulation Library Reference," by Alta Group of Cadence Design Systems, Inc. Product Number: SPW8015, March 1995.

[4] SIMON HAYKIN, "Communication Systems," John Wiley & Sons, INC. 1994, 3rd Edition

[5] Rubén Caballero, "8PSK Signaling over Non-Linear Satellite Channels," Masters Thesis, New Mexico State University, May 1996.

[6] Warren L. Martin and Tien M. Nguyen, "CCSDC - SFCG Efficient Modulation Methods Study, A Comparison of Modulation Schemes, Phase 1: Bandwidth Utilization (Response to SFCG Action Item 12/32)," SFCG-13, Ottawa Canada, 13-21 October 1993, report dated 24 September 1993.

[7] Dr. Manfred Otter, "CCSDC - SFCG Efficient Modulation Methods Study, A Comparison of Modulation schemes, Phase 1b: A Comparison of QPSK, OQPSK, BPSK, and GMSK Modulation Systems (Response to SFCG Action Item 12/32)," European Space Agency/ESOC, Member CCSDS Subpanel 1E, (RF and Modulation), June 1994.

[8] Warren L. Martin and Tien M. Nguyen, "CCSDC - SFCG Efficient Modulation Methods Study, A Comparison of Modulation Schemes, Phase 2: Spectrum Shaping (Response to SFCG Action Item 12/32)," SFCG Meeting, Rothenberg, Germany 14-23 September 1 994, report dated August 1994.

[9] Warren L. Martin, Tien M. Nguyen, Aseel Anabtawi, Sami M. Hinedi, Loc V. Lam and Mazen M. Shihabi, "CCSDC - SFCG Efficient Modulation Methods Study Phase 3: End-to-End System Performance," Jet Propulsion Laboratory, May 1995.

[10] PIL JOONG LEE, " Computation of the Bit Error Rate of Coherent M-ary PSK with Gray code Bit Mapping" IEEE TRANSACTIONS ON COMMUNICATIONS, VOL.COM-34,NO.5,MAY 1986.

[11] Lonnie C. Ludeman, "Fundamentals of Digital Signal Processing," John Wiley & Sons, 1986.

[12] Leon W. Couch II, "Digital and Analog Communication Systems," Macmillan Publishing Company, 1993 , Fourth Edition.

[13] Stephen Horan, "Introduction to PCM Telemetering Systems," CRC Press Inc. 1993.

[14] Alberto Gutierrez Jr., and William Ryan, "Equalization and Detection for Digital Communication Over NonLinear Bandlimited Satellite Communication Channels", Dec 1995, Tech Report # NMSU-ECE-95-008